Received: 29 August 2025 | Revised: 16 April 2026 | Accepted: 18 May 2026 | Published online: 10 June 2026

Journal of Computational and Cognitive Engineering
2026, Vol. 5(3) 438–462
DOI: 10.47852/bonviewJCCE62027466

RESEARCH ARTICLE

An Innovative Exponential Distribution for Modeling Various Risk Trends: Theory, Bayesian Inference, and Applications in Partially Accelerated Life Tests with Dispersion Data

Mohamed S. Eliwa[1,2,*], Mohamed F. Abouelenein[3], Jondeep Das[4], Lakhimi Doley[5], Partha Jyoti Hazarika[5], Gholamhossein G. Hamedani[6] and Ehab M. Almetwally[7]

[1] *College of Science, Qassim University, Saudi Arabia*

[2] *Faculty of Science, Mansoura University, Egypt*

[3] *College of Business, Imam Mohammad Ibn Saud Islamic University (IMSIU), Saudi Arabia*

[4] *Department of Statistics, Bhattadev University, India*

[5] *Department of Statistics, Dibrugarh University, India*

[6] *Department of Mathematical and Statistical Sciences, Marquette University, USA*

[7] *College of Science, Imam Mohammad Ibn Saud Islamic University (IMSIU), Saudi Arabia*

Abstract: This paper presents a new asymmetric generalization of the exponential distribution tailored for non-negative datasets that display unimodal or bimodal characteristics. A shape-controlling parameter substantially improves the model's flexibility, enabling it to accommodate a broader spectrum of distributional shapes compared to the traditional exponential distribution. The theoretical study offers a thorough derivation of essential features, encompassing the moment-generating function, raw moments, mean deviation, entropy measures, and stochastic representations. An in-depth examination of the hazard rate demonstrates its capacity to represent both increasing and bathtub-shaped functions, rendering it especially appropriate for dependability and lifespan data analysis. Additionally, multiple characterization outcomes are produced to reinforce the theoretical foundation, and a modeling framework for partially accelerated life-test conditions is created. Parameter estimation is performed utilizing both conventional and Bayesian inferential methodologies. A thorough simulation analysis assesses the efficacy of these estimators in terms of bias and mean squared error. The model's practical applicability is illustrated through two real-world asymmetric datasets: walking dimension metrics and breast cancer survival durations. Ultimately, likelihood ratio tests are utilized to evaluate the proposed distribution against nested alternatives, consistently demonstrating its enhanced performance and effectiveness in hypothesis testing.

Keywords: statistical model, failure analysis, simulation, Bayesian inference, data analysis

1. Introduction

The exponential distribution holds a pivotal role in probability theory and applied statistics, functioning as a fundamental model across various scientific and technical fields. In reliability engineering, it underpins the modeling of component failures and system lifespans; in survival analysis, it serves as a standard for comprehending mortality trends and treatment impacts; and in queuing theory, it delineates inter-arrival intervals and service durations in stochastic service systems. The extensive utilization of the exponential distribution arises from two primary characteristics: its exceptional mathematical manageability and its unique memoryless quality. The memoryless feature, formally articulated

***Corresponding author:** Mohamed S. Eliwa, College of Science, Qassim University, Saudi Arabia and Faculty of Science, Mansoura University, Egypt. Email: m.eliwa@qu.edu.sa

as $P(X > s + t | X > s) = P(X > t)$ for all $s, t \geq 0$, signifies that the likelihood of enduring for a further time interval is unaffected by the duration already elapsed. This attribute indicates a constant hazard rate, meaning the immediate probability of failure remains consistent across the unit's lifespan. This pattern precisely illustrates situations where the effects of aging are minimal or where failures arise solely from random external shocks rather than progressive decline. Practical applications encompass predicting the duration between radioactive decay occurrences, the intervals of client arrivals in memoryless queuing systems, and the operational lifespans of individual electronic components functioning within their design parameters. Formally, the classical exponential distribution with rate parameter $\lambda > 0$ is characterized by its probability density function (PDF):

$$f(x; \lambda) = \lambda e^{-\lambda x}, \; x > 0, \tag{1}$$

where λ denotes the rate of occurrence or, correspondingly, the inverse of the mean lifetime. The cumulative distribution function (CDF), which measures the chance that a random variable X is less than or equal to a specified value x, is expressed as:

$$F(x; \lambda) = 1 - e^{-\lambda x}, \; x > 0. \tag{2}$$

The survival function, denoting the likelihood that a unit endures beyond time x, is expressed as $S(x; \lambda) = e^{-\lambda x}$, whereas the hazard (or failure rate) function remains constant at $h(x; \lambda) = \lambda$ for all $x > 0$. The constant hazard rate, although technically advantageous, represents both the defining feature and the primary constraint of the exponential model.

Despite its theoretical sophistication and computational ease, the classical exponential distribution possesses inherent restrictions that considerably constrain its applicability to actual lifetime data. The presumption of a constant danger rate seldom applies in real-world scenarios, as empirical data from biological, mechanical, and technological systems continually reveal that hazard functions display dynamic, time-dependent tendencies. In biological systems, the hazard rate often escalates with age due to physiological degradation, accumulation of cellular damage, and the gradual reduction of immunological function. In specific industrial environments, especially regarding electronic components and software systems, the hazard rate may diminish over time when early failures, commonly referred to as "infant mortality," are eradicated during initial operation, resulting in a more resilient surviving population. Many real-world systems prominently display bathtub-shaped hazard functions, which consist of three distinct phases: an initial decreasing hazard phase (burn-in), followed by a relatively stable hazard rate during the useful life, and culminating in an increasing hazard rate during the wear-out phase. This pattern is prevalent in reliability engineering and has been recorded in several applications, such as human mortality studies, mechanical component evaluation, and electronic device reliability assessment. The exponential distribution's fixed hazard rate essentially prevents it from accurately representing these dynamic failure patterns, resulting in significant model misspecification and inaccurate conclusions.

The exponential distribution, in addition to its hazard rate limitations, enforces stringent constraints on the general configuration of the probability distribution. Its PDF is strictly monotonically declining, with a mode at zero and a singular, consistent pattern of decay. This unimodal, monotonically decreasing structure is incapable of accommodating datasets that display internal modes, multimodality, or various levels of skewness. In actuality, lifespan data often exhibit characteristics that significantly diverge from this idealized pattern, including right-skewed distributions with changing tail weights, platykurtic or leptokurtic geometries, and modes positioned away from zero. Moreover, the exponential distribution implicitly presupposes that the underlying population is homogeneous, with all units experiencing identical failure mechanisms at a constant rate. Nonetheless, actual populations are often heterogeneous, consisting of subpopulations with unique failure characteristics due to manufacturing variability, differing operating environments, changes in maintenance procedures, or intrinsic diversity within biological populations. Heterogeneous populations frequently produce intricate failure patterns, characterized by multimodality and heavy tails, which the basic exponential model fails to represent well.

In the last few decades, scholars have come up with different changes and additions to the traditional exponential distribution to get around its limitations. These changes aim to keep the distribution's basic simplicity and ease of understanding while greatly improving its ability to capture the complex patterns found in real-world data. Recent advancements include the α-extended exponential distribution [1], which adds an extra shape parameter to make the distribution more flexible; the unit extended exponential distribution [2], which is designed to model proportions and rates that are limited to the unit interval; and the Topp-Leone extended exponential distribution [3], which combines the exponential baseline with the Topp-Leone family to make it even more flexible. Flexible extensions to extreme value distributions have been suggested, with substantial generalizations put forth by Eliwa et al. [4] and El-Morshedy [5], concentrating on the modeling of severe events and rare failures. Extensions of the Type-II exponential distribution [6] offer additional techniques for modeling unusual hazard behaviors, while the DUS exponential distribution [7] introduces a transformation-based approach for generating new distributional forms. Subsequent developments include the unit moment exponential distribution [8], the log-exponential family [9], the truncated transmuted exponential distribution [10], and various additional extensions to exponential probability distributions [11]. These extensions usually get more flexible by adding extra shape or scale parameters, using transformation techniques, combining with discrete distributions, or using generator families like the Marshall–Olkin, Kumaraswamy, or beta-G frameworks.

A notable deficiency in the conventional exponential distribution literature pertains to the modeling of bimodal data originating from heterogeneous populations or intricate failure mechanisms. Bimodality, characterized by the existence of two distinct modes in a probability distribution, frequently arises in practical applications across various domains, including financial econometrics, actuarial science, income distribution modeling, and industrial engineering. In reliability contexts, bimodal lifetime distributions may emerge when a population consists of two distinct subgroups with varying characteristic lifetimes, when failure mechanisms evolve over time, or when temporal aggregation of data from different operational periods yields composite distributions. To meet these modeling needs, several bimodal distributions have been suggested, such as the bimodal exponential distribution [12], the modified bimodal exponential distribution [13], and the exponentiated exponential distributions [14]. For in-depth discussions on bimodal modeling methodologies and their utilizations, readers should consult References [15, 16]. Simultaneous advancements in the literature concerning asymmetric distributions have yielded significant frameworks for modeling nonstandard data patterns. The skew-normal distribution [17], initially formulated on the real line for asymmetric unimodal data, has been significantly expanded to address bimodal configurations. A particularly elegant approach was proposed by Elal-Olivero et al. [18], who introduced a bimodal normal distribution with the PDF:

$$f(x;\alpha)=\left(\frac{1+\alpha x^2}{1+\alpha}\right)\phi(x),\ x\in\mathbb{R},\ \alpha\geq 0, \tag{3}$$

where $\phi(x)$ is the standard normal density function. This formulation attains bimodality via a polynomial weighting mechanism that maintains analytical tractability, while allowing regulation of the bimodality degree through the parameter α. The distribution becomes the standard normal when $\alpha = 0$. As α gets bigger, the distribution shows more and more bimodal traits.

Even though there is a lot of research on exponential distribution extensions, there are still some important gaps that this study aims to fill. A lot of current models can't naturally handle bimodality while still keeping closed-form expressions for important reliability measures like the hazard function, mean residual life, and quantile function. Analytical tractability is necessary for real-world use, understanding parameters, and working with standard inferential methods. Moreover, the amalgamation of adaptable exponential-type models with sophisticated life testing frameworks has garnered minimal scrutiny in the literature. Partially accelerated life testing (PALT), which combines normal and accelerated operating conditions to efficiently collect failure data, needs distributional assumptions that can accurately capture the complex failure patterns seen at different stress levels. Likewise, progressive censoring schemes, which facilitate the strategic removal of units during testing to enhance resource allocation, necessitate distributions characterized by manageable likelihood functions and dependable estimation methodologies. Also, the mathematical properties that uniquely define a distribution are important theoretical foundations for any probability model, but they are often ignored in applied extensions. These kinds of characterizations provide different ways to check things, show deep structural properties, and make it easier to compare different distributional families. These gaps collectively drive the creation of a more structurally flexible yet mathematically manageable extension of the exponential distribution that meets the varied needs of contemporary reliability analysis.

This research introduces an innovative extension of the exponential distribution, termed the New Extended Exponential (NEExp) distribution, specifically formulated for the analysis of positive datasets that display either unimodal or bimodal traits. The suggested extension modifies the bimodal weighting architecture created by Elal-Olivero et al. [18] for the normal distribution to fit the exponential framework. This makes it a flexible model that can be analyzed for lifetime data. Many of the earlier proposed extensions of the exponential distribution only focus on adding shape parameters to make the distribution more flexible. In contrast, this study makes a bigger contribution to both theoretical development and practical use. The proposed model accommodates various hazard rate shapes, including increasing, decreasing, constant, and bathtub patterns. It also allows for closed-form expressions for several significant statistical and reliability properties, thereby improving its interpretability and practical utility. Besides the development of the distribution, this study presents new characterization results utilizing truncated moments, hazard function structures, and conditional expectations, thereby fortifying the theoretical framework of the model. Moreover, the suggested distribution is methodically incorporated into a Step-Stress Partially Accelerated Life Testing (SS-PALT) framework characterized by progressive Type-II censoring and binomial removals, mirroring authentic industrial testing conditions. From an inferential standpoint, both classical maximum likelihood estimation (MLE) and Bayesian estimation methodologies are formulated, and their efficacy is meticulously assessed and contrasted via comprehensive Monte Carlo simulation studies. This theoretical and applied approach offers a thorough inferential framework that distinctly differentiates the current contribution from previous exponential-type extensions.

PALT has become very popular in reliability analysis because it is a useful way to test product lifetimes when full-scale testing under normal operating conditions is too time-consuming or expensive. In contrast to fully accelerated life testing, which puts all units under extra stress during the whole test, PALT starts testing under normal conditions and then adds acceleration. This gives a balanced method that combines real-world operating data with the benefits of accelerated testing. The step-stress PALT (SS-PALT) model is a very useful version of this method. In this model, test units are first put through normal operating conditions for a set amount of time, called the stress change time (τ). After that, units that survive are put through accelerated stress conditions for the rest of the test. The two-stage structure of SS-PALT makes it possible to collect data quickly and accurately assess reliability in a shorter amount of time. This makes it especially useful in fields like electronics manufacturing, mechanical systems engineering, and medical device development [19, 20]. In SS-PALT, the acceleration mechanism is usually modeled with an acceleration factor $\beta > 1$, which connects the time it takes for something to fail when it is sped up to the time it takes for it to fail when it is normal. Combining SS-PALT with progressive Type-II censoring has more practical benefits because progressive censoring lets you plan to remove surviving units at intermediate failure times, which is useful when you have to deal with cost limits, resource limits, and other practical issues that come up in industrial testing environments. The binomial removal mechanism, in which each surviving unit at a failure time is independently removed with a fixed probability, establishes a probabilistically driven framework that encapsulates uncertain removal decisions and increases model adaptability. The literature has examined analogous frameworks that integrate accelerated life testing with progressive censoring, employing diverse lifetime models; refer to References [21, 22] for examples. The current study augments the existing literature by introducing the innovative NEExp distribution, which offers increased adaptability for modeling various failure behaviors while preserving the analytical feasibility necessary for effective inference in intricate censoring frameworks.

The goal of this paper is to show a new kind of exponential distribution that is meant to better capture the complexities of real-world lifetime data. We expand on the model proposed in Section 2 and discuss it in great detail, including the theoretical reasons for its design. The purpose of this new extension is to provide a more accurate explanation of unimodal and bimodal behavior using non-negative data, as opposed to the standard exponential distribution. Section 3 talks about the new model's distributional properties, especially its statistical and reliability parts. These parts show that the model is more flexible and can be used in more situations than the standard exponential form. Section 4 of the study shows a number of characterization results that were obtained using different analytical methods. This includes methods that use two truncated moments, conditional expectancies, and hazard function forms. These kinds of explanations make the model's theoretical base stronger and make it easier to understand and use in real life. In Section 5, we talk about how to use the MLE method to figure out parameters when you have all the data. This section describes how estimators work and how to use them correctly in real life based on a simulation study. Applying the model to PALT in Section 6 broadens the study's scope. We use both Bayesian and MLE methods to make educated guesses about the parameters. This means that the method works well when you don't have much time and need to test something quickly, and simulation studies are done. Mean squared error (MSE) and bias are two ways to measure how accurate an estimator is. This helps us understand how well they work in different situations. In the end, Section 7 uses real-world datasets to put the model into action for both complete and censored schemes. The likelihood ratio test (LRT) is then used to compare its performance to similar or nested models. The empirical results demonstrate that intricate lifespan data displaying diverse hazard rate patterns can be more accurately approximated utilizing the proposed distribution. In Section 8, we give our final thoughts.

2. A New Mathematical Formulation of the Exponential Distribution Extension

Let X be a continuous random variable. The PDF of the newly proposed extended exponential distribution, referred to as the NEExp distribution, is given by:

$$f(x;\alpha,\lambda)=\frac{\lambda\left(1+\alpha x^2\right)}{C(\alpha,\lambda)}e^{-\lambda x},\ x>0,\ \lambda>0,\ \alpha\geq 0, \quad (4)$$

where $C(\alpha,\lambda)$ is a normalizing constant defined as:

$$C(\alpha,\lambda)=1+\frac{2\alpha}{\lambda^2}.$$

We denote this as $X\sim \mathrm{NEExp}(\alpha,\lambda)$. Notably, when $\alpha=0$, the NEExp distribution reduces to the standard exponential distribution with rate parameter λ. The parameter $\alpha\geq 0$ plays a crucial role in controlling the shape, asymmetry, and tail behavior of the proposed $\mathrm{NEExp}(\alpha,\lambda)$ distribution. In particular, when $\alpha=0$, the density function reduces to the classical exponential distribution with rate parameter λ, thereby showing that the proposed model is a genuine extension of the exponential family. For $\alpha>0$, the multiplicative term $(1+\alpha x^2)$ modifies the standard exponential kernel $e^{-\lambda x}$ by introducing a quadratic component in x, which increases the flexibility of the model. As α increases, the contribution of the term αx^2 becomes more dominant, resulting in heavier right tails, increased dispersion, and greater deviation from the constant hazard structure of the exponential model. This modification directly impacts higher-order moments, as evident from the expressions of the variance, skewness, and kurtosis, all of which are increasing functions of α. Consequently, the parameter α governs the degree of asymmetry and peakedness of the distribution. Furthermore, the first derivative of the density function shows that the number and location of critical points depend explicitly on α, allowing the distribution to exhibit either unimodal or bimodal behavior depending on its magnitude relative to λ. Hence, α acts as a shape-controlling parameter that determines whether the density maintains a single peak (similar to the exponential case) or develops an additional turning point, thereby producing bimodality. This enhanced structural flexibility makes the NEExp distribution particularly suitable for modeling asymmetric lifetime data with varying dispersion and non-monotonic hazard rate patterns. The CDF of the $\mathrm{NEExp}(\alpha,\lambda)$ distribution is given by:

$$F(x;\alpha,\lambda)=1+\frac{e^{-\lambda x}\left[-\lambda^2-\alpha\{2+x\lambda(\lambda x+2)\}\right]}{2\alpha+\lambda^2};\quad x>0,\ \lambda>0,\ \alpha\geq 0. \quad (5)$$

To derive the CDF from the PDF defined in Equation (4), we integrate the PDF from 0 to x as follows:

$$\begin{aligned}F(x;\alpha,\lambda)&=\int_0^x f(t;\alpha,\lambda)\,dt\\&=\frac{\lambda}{C(\alpha,\lambda)}\left[\int_0^x e^{-\lambda t}\,dt+\alpha\int_0^x t^2e^{-\lambda t}\,dt\right]\\&=\frac{\lambda}{C(\alpha,\lambda)}\left[I_1+\alpha I_2\right],\end{aligned}$$

where I_1 and I_2 are defined as:

$$I_1=\int_0^x e^{-\lambda t}\,dt=\frac{1-e^{-\lambda x}}{\lambda},$$

$$I_2=\int_0^x t^2e^{-\lambda t}\,dt=\frac{1}{\lambda^3}\left\{2+e^{-\lambda x}\left[-\lambda x(\lambda x+2)-2\right]\right\}.$$

Substituting I_1 and I_2 into the expression for $F(x;\alpha,\lambda)$, and simplifying the result, we obtain the final closed-form expression for the CDF of the $\mathrm{NEExp}(\alpha,\lambda)$ distribution.

To provide a clearer understanding of the behavior of the proposed distribution, Figures 1 and 2 illustrate the shapes of the PDF and CDF of the $\mathrm{NEExp}(\alpha,\lambda)$ model for various parameter values. Figure 1 demonstrates that the PDF of the $\mathrm{NEExp}(\alpha,\lambda)$ distribution is highly flexible and capable of exhibiting both unimodal and bimodal shapes depending on the choice of the parameter α. For smaller values of α, the distribution behaves similarly to the classical exponential distribution, displaying a monotonically decreasing shape. However, as α increases, the density can develop a pronounced peak and may even exhibit bimodality, indicating its ability to capture more complex data structures. Additionally, the parameter λ controls the rate of decay, where larger values of λ result in a steeper decline of the density function. Again, Figure 2 presents the corresponding CDFs of the $\mathrm{NEExp}(\alpha,\lambda)$ distribution. The plots show that the CDF remains a smooth and monotonically increasing function for all parameter choices, as expected. Variations in α and λ influence the rate at which the distribution accumulates probability. In particular, larger values of λ lead to faster convergence of the CDF toward unity, while changes in α adjust the curvature, reflecting differences in dispersion and tail behavior.

3. Distributional Properties

3.1. Unimodality and bimodality properties

The $NEExp(\alpha,\lambda)$ distribution can exhibit at most two modes. To determine the number of modes, we differentiate the PDF given in Equation (4) with respect to x:

$$f'(x;\alpha,\lambda)=\frac{-\lambda^3e^{-\lambda x}\left(\lambda+\alpha\lambda x^2-2\alpha x\right)}{2\alpha+\lambda^2}.$$

Figure 1
The PDF for different parameter choices

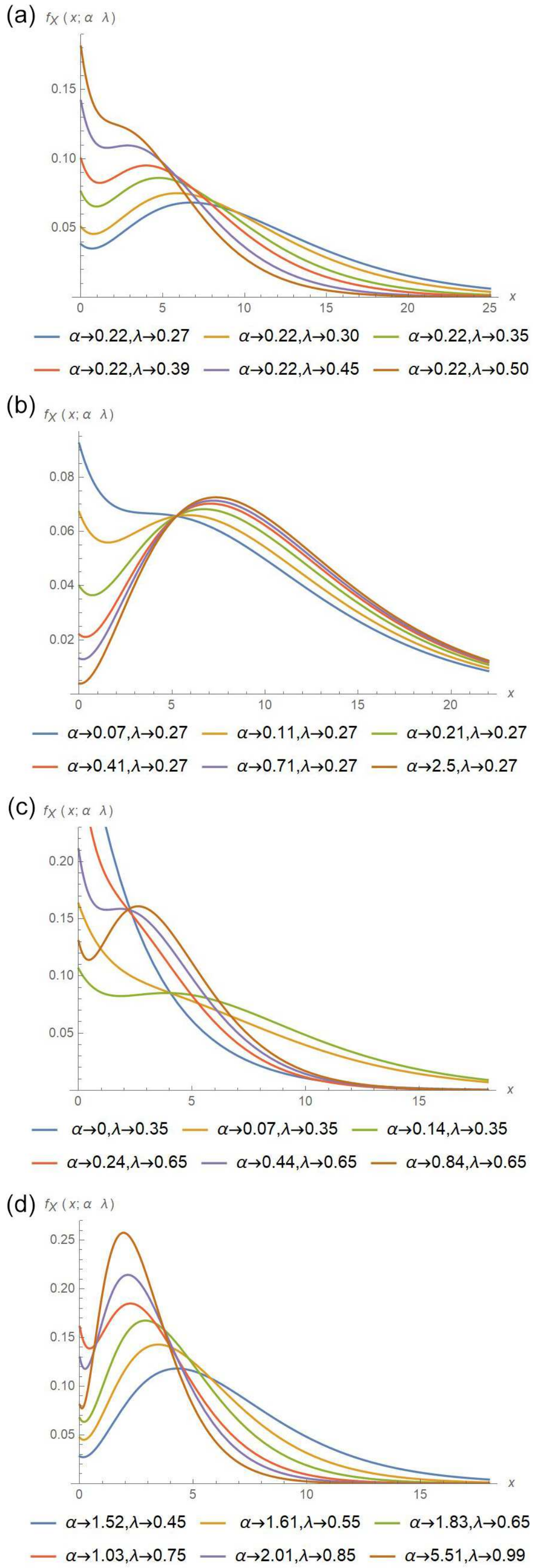

Setting the derivative equal to zero, we solve for the critical points:

$$\lambda + \alpha\lambda x^2 - 2\alpha x = 0.$$

This yields a quadratic equation in x, which may have at most two real roots. Therefore, the density function $f(x;\alpha,\lambda)$ can have at most two turning points, implying that the $NEExp(\alpha,\lambda)$ distribution is at most bimodal.

Figure 2
The CDF for different parameter choices

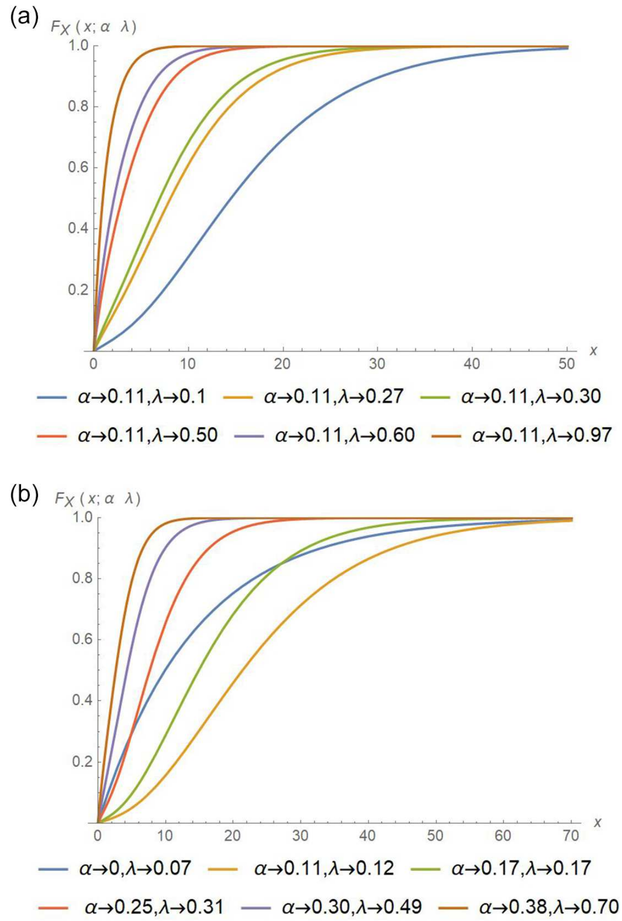

3.2. Moment-generating function

The moment-generating function (MGF) of the NEExp(α,λ) distribution is given by:

$$M(t) = \frac{\lambda\left(2\alpha + (t-\lambda)^2\right)}{C(\alpha,\lambda)(\lambda - t)^3}, \tag{6}$$

where $C(\alpha,\lambda) = 1 + \frac{2\alpha}{\lambda^2}$ is the normalizing constant defined previously. Using the PDF provided in Equation (4), the MGF of a random variable $X \sim$ NEExp(α,λ) is defined as:

$$M(t) = \mathbb{E}[e^{tX}] = \int_0^\infty e^{tx} f(x;\alpha,\lambda)\,dx$$

$$= \frac{\lambda}{C(\alpha,\lambda)}\left[\int_0^\infty e^{-\lambda x+tx}\,dx + \alpha\int_0^\infty x^2 e^{-\lambda x+tx}\,dx\right]$$

$$= \frac{\lambda}{C(\alpha,\lambda)}\left[I_3 + \alpha I_4\right],$$

where I_3 and I_4 represent the following integrals:

$$I_3 = \int_0^\infty e^{-(\lambda-t)x}\,dx = \frac{1}{\lambda-t}, \text{ (validfor} t < \lambda),$$

$$I_4 = \int_0^\infty x^2 e^{-(\lambda-t)x}\,dx = \frac{2}{(\lambda-t)^3}.$$

Substituting I_3 and I_4 back into the MGF expression, we obtain:

$$M(t) = \frac{\lambda}{C(\alpha,\lambda)}\left[\frac{1}{\lambda - t} + \alpha \cdot \frac{2}{(\lambda - t)^3}\right] = \frac{\lambda\left(2\alpha + (t-\lambda)^2\right)}{C(\alpha,\lambda)(\lambda - t)^3}.$$

Considering (it) instead of t in Equation (6), the characteristic function of the $NEExp(\alpha,\lambda)$ distribution is obtained and is given by:

$$\phi(t) = \frac{\lambda\left(2\alpha + (it-\lambda)^2\right)}{C(\alpha,\lambda)(\lambda - it)^3}. \tag{7}$$

Taking the natural logarithm on both sides of Equation (6), the cumulant generating function of the $NEExp(\alpha,\lambda)$ distribution is derived as:

$$K(t) = \log\lambda + \log\left[2\alpha + (t-\lambda)^2\right] - \log C(\alpha,\lambda) - 3\log(\lambda - t). \tag{8}$$

3.3. Stochastic representation

The extended exponential distribution can be expressed as a mixture of an exponential distribution and an Erlang distribution. This stochastic representation provides insight into the structural composition of the distribution. Let X be a random variable following the extended exponential distribution with parameters $\lambda > 0$ and α. Then X admits the following stochastic representation:

$$X = \begin{cases} Y_1 & \text{with probability } \frac{\lambda^2}{\lambda^2 + 2\alpha}, \\ Y_2 & \text{with probability } \frac{2\alpha}{\lambda^2 + 2\alpha}, \end{cases}$$

where $Y_1 \sim \text{Exponential}(\lambda)$ and $Y_2 \sim \text{Erlang}(3,\lambda)$. Here, Y_1 and Y_2 are independent. To verify this representation, we compute the MGF of the mixture and show it matches the given MGF of X. The MGF of $Y_1 \sim \text{Exponential}(\lambda)$ is:

$$M_{Y_1}(t) = \frac{\lambda}{\lambda - t}, \; t < \lambda.$$

The MGF of $Y_2 \sim \text{Erlang}(3,\lambda)$ is:

$$M_{Y_2}(t) = \left(\frac{\lambda}{\lambda - t}\right)^3, \; t < \lambda.$$

The MGF of the mixture X is a weighted sum of $M_{Y_1}(t)$ and $M_{Y_2}(t)$:

$$\begin{aligned} M_X(t) &= \frac{\lambda^2}{\lambda^2 + 2\alpha} \cdot \frac{\lambda}{\lambda - t} + \frac{2\alpha}{\lambda^2 + 2\alpha} \cdot \left(\frac{\lambda}{\lambda - t}\right)^3 \\ &= \frac{\lambda^3}{\lambda^2 + 2\alpha}\left[\frac{1}{\lambda - t} + \frac{2\alpha}{(\lambda - t)^3}\right] \\ &= \frac{\lambda\left(2\alpha + (t-\lambda)^2\right)}{C(\alpha,\lambda)(\lambda - t)^3}. \end{aligned}$$

This matches the original MGF provided for the extended exponential distribution. Thus, the stochastic representation is valid. Although the NEExp(α,λ) distribution admits a stochastic representation as a two-component mixture of an exponential(λ) and an Erlang$(3,\lambda)$ distribution, it is fundamentally different from conventional finite mixture models. In standard mixture formulations, the mixing proportions and component parameters are treated as independent free parameters, which may lead to issues such as overparameterization, lack of identifiability, and computational instability during estimation. In contrast, the proposed NEExp model provides a unified and parsimonious formulation governed by only two parameters (α,λ). The mixing weights are not arbitrary but are fully determined by the model parameters, specifically $\frac{\lambda^2}{\lambda^2 + 2\alpha}$ and $\frac{2\alpha}{\lambda^2 + 2\alpha}$, while both components share a common scale parameter λ. This structural constraint ensures identifiability and avoids label-switching problems typically encountered in mixture models. Moreover, the NEExp distribution retains analytical tractability, with closed-form expressions available for its CDF, MGF, moments, and hazard rate. Such explicit forms are generally unavailable in standard mixture distributions. Therefore, the NEExp model should be viewed as a structured mixture distribution that achieves a balance between flexibility and parsimony, providing practical advantages in both theoretical analysis and statistical inference.

3.4. Elementary moments and analytical indicators

The r^{th} raw moment of the $NEExp(\alpha,\lambda)$ distribution is expressed as:

$$E(X^r) = \frac{1}{(2\alpha + \lambda^2)}\left[\lambda^{-r}\left\{\lambda^2 + \alpha(r+1)(r+2)\right\}\Gamma(r+1)\right]. \tag{9}$$

Using the PDF defined in Equation (4), the r^{th} order moment can be derived as:

$$\begin{aligned} E(X^r) &= \int_0^\infty x^r f(x;\alpha,\lambda)dx \\ &= \frac{\lambda}{C(\alpha,\lambda)}\left[\int_0^\infty x^r e^{-\lambda x}dx + \alpha\int_0^\infty x^{r+2}e^{-\lambda x}dx\right] \\ &= \frac{\lambda}{C(\alpha,\lambda)}\left[I_5 + I_6\right], \end{aligned}$$

where I_5 is the r^{th} moment of the exponential distribution, and I_6 is computed as:

$$I_6 = \int_0^\infty x^{r+2}e^{-\lambda x}dx = \lambda^{-r-3}\Gamma(r+3).$$

Thus, substituting the values of I_5 and I_6 yields:

$$E(X^r) = \frac{1}{(2\alpha + \lambda^2)}\left[\lambda^{-r}\left\{\lambda^2 + \alpha(r+1)(r+2)\right\}\Gamma(r+1)\right].$$

By substituting $r = 1,2,3,4$ into Equation (9), we obtain the first four raw moments of the $NEExp(\alpha,\lambda)$ distribution:

$$E[X] = \frac{6\alpha + \lambda^2}{\lambda(2\alpha + \lambda^2)}, \; E[X^2] = \frac{2(12\alpha + \lambda^2)}{\lambda^2(2\alpha + \lambda^2)},$$

$$E[X^3] = \frac{6(20\alpha + \lambda^2)}{\lambda^3(2\alpha + \lambda^2)}, \; E[X^4] = \frac{24(30\alpha + \lambda^2)}{\lambda^4(2\alpha + \lambda^2)}.$$

Using the raw moments, the variance of X is calculated as:

$$\text{Var}(X) = \frac{12\alpha^2 + 16\alpha\lambda^2 + \lambda^4}{\left(2\alpha\lambda + \lambda^3\right)^2}.$$

Furthermore, the coefficients of skewness (γ_1) and kurtosis (γ_2) of the $NEExp(\alpha,\lambda)$ distribution are derived as:

$$\gamma_1 = \frac{2\left[\lambda^6 + 30\alpha\lambda^4 + 36\alpha^2\lambda^2 + 24\alpha^3\right]}{\left(\lambda^4 + 16\alpha\lambda^2 + 12\alpha^2\right)^{3/2}},$$

$$\gamma_2 = \frac{24\left[\lambda^8 + 60\alpha\lambda^6 + 180\alpha^2\lambda^4 + 240\alpha^3\lambda^2 + 120\alpha^4\right]}{\left(\lambda^4 + 16\alpha\lambda^2 + 12\alpha^2\right)^2}.$$

3.5. Distribution of ordered random variables

The PDF of the i^{th} order statistic for the $NEExp(\alpha, \lambda)$ distribution is obtained by:

$$f_{i:n}(x) = \sum_{k=i}^{n} \sum_{l=0}^{n-k} \sum_{m=0}^{\infty} \binom{n}{k}\binom{n-k}{l}\binom{k+l}{m} \frac{(-1)^{l+m}}{A^m}$$

$$\left[mg(x)^{m-1}e^{-m\lambda x}\{g'(x) - \lambda g(x)\}\right]. \quad (10)$$

A random sample $X_1, X_2, \ldots, X_n$ is considered from the PDF given in (4), and the associated order statistics are $X_{1:n} < X_{2:n} < \ldots < X_{n:n}$. Then, the CDF of the i^{th} order statistic is defined as:

$$F_{i:n}(x) = \sum_{k=i}^{n} (nk)\, F(x)^k[1 - F(x)]^{n-k}$$

$$= \sum_{k=i}^{n} \sum_{l=0}^{n-k} (-1)^l\,(nk)\,(n-kl)$$

$$[1 + \frac{e^{-\lambda x}[-\lambda^2 - \alpha 2 + x\lambda(\lambda x + 2)]}{2\alpha + \lambda^2}]^{k+l}.$$

$$= \sum_{k=i}^{n} \sum_{l=0}^{n-k} (-1)^l\,(nk)\,(n-kl)\,F(x)^{k+l}$$

Define the following:

$$A = 2\alpha + \lambda^2, g(x) = \lambda^2 + \alpha\,(2 + x\lambda(\lambda x + 2)),$$

$$z(x) = \frac{-g(x) \cdot e^{-\lambda x}}{A}.$$

Then,

$$[1 + z(x)]^{k+l} = \sum_{m=0}^{\infty} (lk + lmt)z(x)^m$$

$$= \sum_{m=0}^{\infty} (lk + lm)\left(\frac{-g(x) \cdot e^{-\lambda x}}{A}\right)^m$$

$$[1 + z(x)]^{k+l} = \sum_{m=0}^{\infty} lk + lm)z(x)^m$$

$$= \sum_{m=0}^{\infty} (lk + lm)(\frac{-g(x) \cdot e^{-\lambda x}}{A})^m$$

$$= \sum_{m=0}^{\infty} (lk + lm) \cdot \frac{(-1)^m}{A^m} \cdot g(x)^m \cdot e^{-m\lambda x}.$$

Hence, the CDF of the i^{th} order statistic is expressed as

$$F_{i:n}(x) = \sum_{k=i}^{n} \sum_{l=0}^{n-k} \sum_{m=0}^{\infty} (lnkt)(ln - kl)t(lk + lm)$$
$$\frac{(-1)^{l+m}}{A^m} \cdot g(x)^m \cdot e^{-m\lambda x}.$$

Differentiating the CDF with respect to x, the PDF of the i^{th} order statistic becomes

$$f_{i:n}(x) = \frac{d}{dx}F_{i:n}(x)$$

$$= \sum_{k=i}^{n} \sum_{l=0}^{n-k} \sum_{m=0}^{\infty} (lnk)(ln - kl)(lk + \mathrm{l}m)\frac{(-1)^{l+m}}{A^m}$$
$$\left[mg(x)^{m-1}e^{-m\lambda x}\{g'(x) - \lambda g(x)\}\right].$$

3.6. Measure of average dispersion

The mean deviation (MD) of the $NEExp(\alpha, \lambda)$ distribution around the mean μ is given by

$$\mu_1(x) = \frac{1}{\lambda(2\alpha + \lambda^2)}[2\alpha\lambda\mu - 6\alpha + \lambda^3\mu - \lambda^2 \quad (11)$$

$$+ 2e^{-\lambda\mu}\{\alpha(\lambda\mu(\lambda\mu + 4) + 6) + \lambda^2\}], \quad (12)$$

where the MD about the mean μ is defined as

$$\mu_1(x) = \int_0^{\infty} |x - \mu| f(x; \alpha, \lambda)\,dx$$

$$= \int_0^{\mu} (\mu - x)f(x; \alpha, \lambda)\,dx$$

$$+ \int_{\mu}^{\infty} (x - \mu)f(x; \alpha, \lambda)\,dx = I_7 + I_8.$$

Now, the integrations I_7 and I_8 are evaluated as:

$$I_7 = \int_0^{\mu} (\mu - x)f(x; \alpha, \lambda)\,dx$$

$$= \frac{1}{C(\alpha,\lambda)}\left[\int_0^{\mu} (\mu - x)e^{-\lambda x}\,dx + \alpha\int_0^{\mu} (\mu - x)x^2e^{-\lambda x}\,dx\right]$$

$$= \frac{1}{C(\alpha,\lambda)}\left[\frac{\lambda\mu + e^{-\lambda\mu} - 1}{\lambda^2} + \frac{\alpha e^{-\lambda\mu}\left(2e^{\lambda\mu}(\lambda\mu - 3) + \lambda\mu(\lambda\mu + 4) + 6\right)}{\lambda^4}\right].$$

In a similar way, I_8 is calculated as

$$I_8 = \int_{\mu}^{\infty} (x - \mu)f(x; \alpha, \lambda)\,dx$$

$$= \frac{1}{C(\alpha,\lambda)}\left[\int_{\mu}^{\infty} (x - \mu)e^{-\lambda x}\,dx + \alpha\int_{\mu}^{\infty} (x - \mu)x^2e^{-\lambda x}\,dx\right]$$

$$= \frac{1}{C(\alpha,\lambda)}\left[\frac{e^{-\lambda\mu}}{\lambda^2} + \frac{e^{-\lambda\mu}(\lambda\mu(\lambda\mu + 4) + 6)}{\lambda^4}\right].$$

Combining the results of I_7 and I_8, the final expression for the MD about the mean μ can be derived. Replacing the mean μ by the median M in Equation (12), the MD about the median for the $NEExp(\alpha, \lambda)$ model can also be provided.

3.7. Entropy metric

The Renyi entropy of the $NEExp(\alpha, \lambda)$ distribution is given by

$$H(x) = \frac{1}{1-\gamma}[\log K(\alpha) - (1 + 2k)$$
$$\log(\gamma\lambda) + \log\Gamma(1 + 2k)], \quad (13)$$

Where:

$$K(\alpha) = \frac{\lambda^\gamma}{C(\alpha,\lambda)^\gamma}\sum_{k=0}^{\infty}\binom{\gamma}{k}\alpha^k.$$

To find the Renyi entropy of order $\gamma > 0$, $\gamma \neq 1$ for a PDF $f(x)$, the formula is:

$$H(x) = \frac{1}{1-\gamma}\log\left(\int f(x)^\gamma\,dx\right).$$

Now, using the PDF defined in Equation (4), the integral involved in the entropy measure is calculated as:

$$\int_0^{\infty} \frac{\lambda^{\gamma}}{C(\alpha,\lambda)^{\gamma}}(1+\alpha x^2)^{\gamma} e^{-x\lambda\gamma} dx$$
$$= \frac{\lambda^{\gamma}}{C(\alpha,\lambda)^{\gamma}} \sum_{k=0}^{\infty} (l\gamma k)\alpha^k \int_0^{\infty} x^{2k} e^{-x\lambda\gamma} dx$$
$$= K(\alpha)(\gamma\lambda)^{-1-2k}\Gamma(1+2k).$$

Hence, the final expression of the Renyi entropy for the proposed distribution can be calculated.

3.8. Reliability properties

This subsection provides some important reliability properties of the newly proposed exponential distribution. The survival function of the $NEExp(\alpha,\lambda)$ distribution is calculated as:

$$S(x;\,\alpha,\,\lambda) = \frac{e^{-\lambda x}\{\lambda^2 + \alpha(\lambda x(\lambda x + 2) + 2)\}}{2\alpha + \lambda^2}; \quad x > 0,\ \lambda > 0,\ \alpha \geq 0. \tag{14}$$

A graphical representation of the survival function for the $NEExp(\alpha,\lambda)$ distribution with different parameter values is shown in Figure 3. From Figure 3(a), it can be observed that increasing λ corresponds to a faster failure rate or shorter lifetime. Moreover, Figure 3 illustrates that increasing both parameters results in the survival function decreasing more rapidly, indicating shorter survival times. The hazard rate function (HRF) of the $NEExp(\alpha,\lambda)$ distribution is given by:

Figure 3
Survival function for different parameter choices

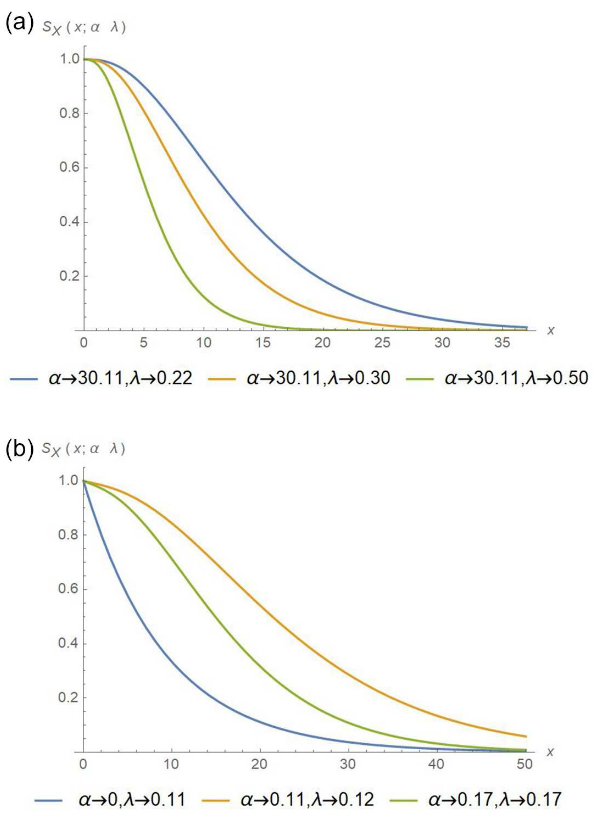

$$h(x;\,\alpha,\,\lambda) = \frac{\lambda^3(\alpha x^2 + 1)}{\lambda^2 + \alpha(\lambda^2 x^2 + 2\lambda x + 2)}; \quad x > 0,\ \lambda > 0,\ \alpha \geq 0. \tag{15}$$

The HRF is graphically listed in Figure 4. From Figure 4(a), a bathtub-shaped HRF is observed, indicating that higher values of λ lead to earlier aging effects, a shorter reliable lifespan, and a higher risk of failure in the long term. Such behavior is typical in many engineering systems, biomedical devices, and industrial products. Furthermore, Figure 4(b) shows how increasing the value of α and decreasing λ can reduce and delay the hazard, thereby making the system more reliable over time. Additionally, the inverse HRF of the $NEExp(\alpha,\lambda)$ distribution can be obtained by taking the reciprocal of $h(x;\alpha,\lambda)$ as given in Equation (15).

4. Characterization of Distribution: Truncated Moments, Risk Function, and Conditional Expectation

4.1. Characterizations based on two truncated moments

This subsection deals with the characterizations of $NEExp$ distribution based on a relationship between two truncated

Figure 4
HRF for different parameter choices

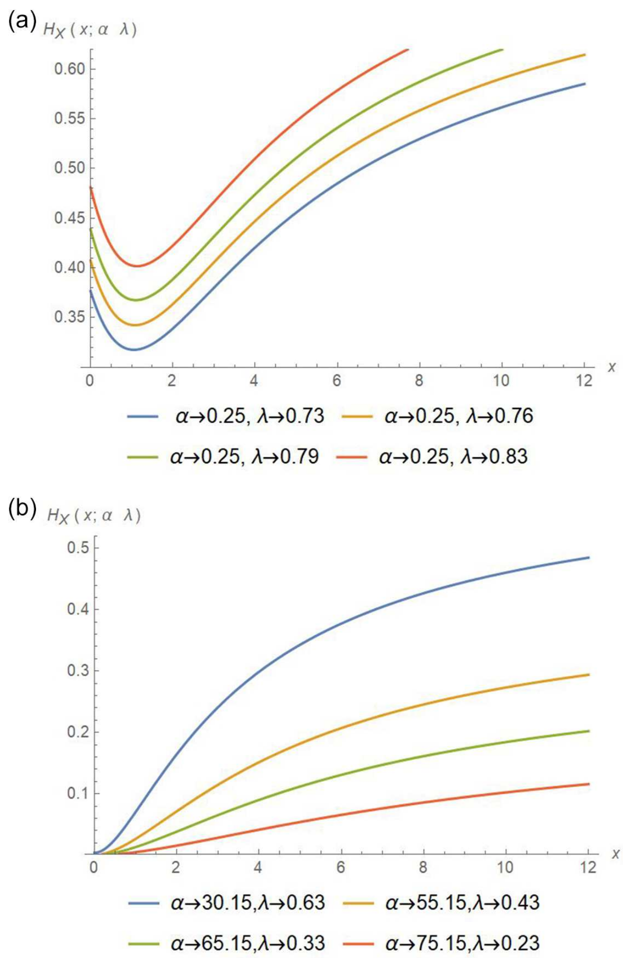

moments. The first characterization applies a theorem of Glanzel [23] Theorem 3.1 given below. Clearly, the result holds as well when the H is not a closed interval. This characterization is stable in the sense of weak convergence.

Theorem 1. Let $(\Omega, \mathscr{F}, \mathbf{P})$ be a given probability space, and let $H = [d, e]$ be an interval for some $d < e$ $(d = -\infty, e = \infty \text{ mightaswellbeallowed})$. Let $X : \Omega \to H$ be a continuous random variable with the distribution function F, and let k and h be two real functions defined on H such that

$$\mathbf{E}[k(X)|X \geq x] = \mathbf{E}[h(X)|X \geq x]\,\eta(x),\ x \in H,$$

is defined with some real function η. Assume that $k, h \in C^1(H)$, $\eta \in C^2(H)$, and F are twice continuously differentiable and strictly monotone functions on the set H. Finally, assume that the equation $\eta h = k$ has no real solution in the interior of H. Then F is uniquely determined by the functions k, h, and η, particularly

$$F(x) = \int_a^x C\left|\frac{\eta'(u)}{\eta(u)\,h(u) - k(u)}\right| \exp(-s(u))\,du,$$

where the function s is a solution of the differential equation $s' = \frac{\eta' h}{\eta h - k}$ and C is the normalization constant, such that $\int_H dF = 1$. The goal is to have $\eta(x)$ as simple as possible.

Proposition 1. *Let the random variable* X*:* $\Omega \to (0, \infty)$ *be continuous, and let* $h(x) = \left(1 + \alpha x^2\right)^{-1}$ *and* $k(x) = h(x)\,e^{-\lambda x}$ *for* $x > 0$*. Then, the density of* X *is given in* (4) *if and only if the function* η *defined in Theorem 3.1 is*

$$\eta(x) = \frac{1}{2}e^{-\lambda x},\ x > 0.$$

Proof. If X has PDF (4), then

$$(1 - F(x))\,E[h(X)|X \geq x] = \textstyle\int_x^\infty Ce^{-\lambda u}du$$

$$= \tfrac{C}{\lambda}e^{-\lambda x},\ x > 0,$$

and

$$(1 - F(x))\,E[k(X)|X \geq x] = \textstyle\int_x^\infty Ce^{-2\lambda u}du$$

$$= \tfrac{C}{2\lambda}e^{-2\lambda x},\ x > 0,$$

and finally

$$\eta(x)\,h(x) - k(x) = -\frac{1}{2}h(x)\,e^{-\lambda x} < 0 \ \mathit{for}\ x > 0.$$

Conversely, if η has the above form, then

$$s'(x) = \frac{\eta'(x)\,h(x)}{\eta(x)\,h(x) - k(x)} = \lambda,$$

and hence

$$s(x) = \lambda x,\ x > 0.$$

In view of Theorem 3.1, X has PDF (4).

Corollary 1. If $X : \Omega \to (0, \infty)$ is a continuous random variable and $h(x)$ is as in Proposition 1. Then, X has PDF (4) if and only if there exist functions k and η defined in Theorem 3.1 satisfying the following first-order differential equation

$$\frac{\eta'(x)\,h(x)}{\eta(x)\,h(x) - k(x)} = \lambda.$$

Corollary 2. The general solution of the differential equation in Corollary 3.1.1 is

$$\eta(x) = e^{\lambda x}\left[-\int \lambda e^{-\lambda x}(h(x))^{-1}k(x) + D\right],$$

where a constant D is used.

Proof. It is obvious that the differential equation is true if X has PDF (4). In the event that the differential equation is valid, then

$$\eta'(x) = \lambda\eta(x) - \lambda(h(x))^{-1}k(x),$$

or

$$\frac{d}{dx}\left\{e^{-\lambda x}\eta(x)\right\} = -\lambda e^{-\lambda x}(h(x))^{-1}k(x),$$

from which we have

$$\eta(x) = e^{\lambda x}\left[-\int \lambda e^{-\lambda x}(h(x))^{-1}k(x) + D\right].$$

It should be noted that Proposition 1 with $D = 0$ presents a collection of functions that fulfill this differential equation. It is evident that additional triplets (h, k, η) meet the requirements of Theorem 3.1.

4.2. Characterization in terms of hazard function

The following first-order differential equation is satisfied by the hazard function, h_F, of a twice differentiable distribution function, F,

$$\frac{f'(x)}{f(x)} = \frac{h_F'(x)}{h_F(x)} - h_F(x).$$

It should be noted that the aforementioned equation is the sole differential equation available in terms of the hazard function for a large number of univariate continuous distributions. We provide nontrivial characterizations of the new distributions in terms of the hazard function in this subsection; these are not the trivial form mentioned above.

Proposition 2. For example X: $\Omega \to (0, \infty)$ *Let* be a random, continuous variable. For the random variable X, PDF (4) *exists. Only if its hazard function* h_F(x) satisfies the differential equation that follows:

$$h_F'(x) - \tfrac{2\alpha x}{1+\alpha x^2}h_F(x) = \lambda^3\left(1 + \alpha x^2\right)\tfrac{d}{dx}$$
$$\left\{\left[\lambda^2 + \alpha(2 + \lambda(2 + \lambda x))\right]^{-1}\right\},\ x > 0,$$

when the boundary condition is applied as $\lim_{x\to 0}h_F(x) = \frac{\lambda^3}{2\alpha+\lambda^2}$.

Proof. Both sides of the equation above are multiplied by $\left(1 + \alpha x^2\right)^{-1}$, we have

$$\frac{d}{dx}\left\{\left(1 + \alpha x^2\right)^{-1}h_F(x)\right\} = \lambda^3\frac{d}{dx}\left\{\left[\lambda^2 + \alpha(2 + \lambda(2 + \lambda x))\right]^{-1}\right\},$$

or

$$h_F(x) = \lambda^3\left(1 + \alpha x^2\right)\left[\lambda^2 + \alpha(2 + \lambda(2 + \lambda x))\right]^{-1},$$

which is the hazard function corresponding to the PDF (4).

4.3. A conditional expectation-based characterization approach

Using a single function ψ of X, we describe the distribution of X in this subsection using the truncated moment of $\psi(X)$. We will simply express the following assertion, which can be used to characterize the *NEExp* distribution, since it has previously been mentioned in Reference [24].

Proposition 3.Let X: Ω → (e, f) be a continuous random variable with CDF F, and let be a differentiable function on (e, f) with $\lim_{x\to f}$.Then for

$$E[\psi(X)|X \le x] = \delta\psi(x),\ x \in (e,f),$$

if and only if

$$\psi(x) = (F(x))^{\frac{1}{\delta}-1},\ x \in (e,f)$$

For $(e,f) = (0,\infty)$, $\psi(x) = \frac{\left[\lambda^2 + \alpha(2+\lambda(2+\lambda x))\right]^{1/\lambda} e^{-x}}{(2\alpha+\lambda^2)^{1/\lambda}}$, $\delta = \frac{\lambda}{\lambda+1}$, Proposition H provides a characterization of the distribution (4).

5. Evaluating Classical Estimators Under Complete Data Through Theory and Simulation

Let $y_1, y_2, \ldots y_n$ be a random sample of size n selected from the $NEExp(\alpha,\lambda)$ distribution. Following this, the log-likelihood function for the collection of parameters $\theta = (\alpha,\lambda)$ is provided by

$$\begin{aligned} l(\theta) &= n\log\lambda + \sum_{i=1}^{n} \log(\alpha y_i^2 + 1) \\ &-\lambda \sum_{i=1}^{n} y_i - n\log\left(\frac{2\alpha}{\lambda^2}+1\right), \end{aligned} \tag{16}$$

Now, the Equation (16) is differentiated for the parameters (α,λ), and log-likelihood equations are now generated as:

$$\frac{\partial \ell}{\partial \lambda} = \frac{n}{\lambda} - \sum_{i=1}^{n} x_i + \frac{4n\alpha}{\lambda^3\left(\frac{2\alpha}{\lambda^2}+1\right)} = 0, \frac{\partial \ell}{\partial \alpha} = \sum_{i=1}^{n} \frac{x_i^2}{\alpha x_i^2+1} - \frac{2n/\lambda^2}{\frac{2\alpha}{\lambda^2}+1} = 0.$$

It is evident that the log-likelihood equations derived above do not have closed-form solutions. As a result, solving them analytically is not feasible. Hence, a numerical optimization strategy employing the GenSA package in R is used to obtain the parameter estimates effectively. A simulation experiment was carried out to evaluate how well the maximum likelihood estimators (MLEs) perform for estimating the parameters of the $NEExp(\alpha,\lambda)$ distribution. For this purpose, random samples were generated using the corresponding quantile function. This process was replicated 1000 times for each of the three selected sample sizes: n = 100, 300, 500 The GenSA optimization package in R was used to calculate the MLEs for each generated sample. Two main criteria were used to assess the estimates' accuracy: bias and MSE [25]. The findings are displayed in Tables 1, 2, and 3, which demonstrate that the MLEs produce precise estimates of the model parameters. Additionally, the asymptotic consistency of the MLEs for the

Table 1
Bias and MSE of MLEs for different values of α with $\lambda = 1$

α	n	λ		α	
		Bias	MSE	Bias	MSE
0	100	0.0734	0.0835	–0.0912	0.0753
	300	–0.0605	0.0697	0.0853	0.0722
	500	0.0389	0.0639	0.0635	0.0678
0.5	100	–0.0644	0.0689	–0.0479	0.0912
	300	0.0565	0.0631	–0.0423	0.0885
	500	0.0503	0.0602	0.0401	0.0791
1	100	–0.0328	0.0643	–0.1521	0.0933
	300	–0.0187	0.0604	0.1224	0.0712
	500	0.0102	0.0389	0.0733	0.0681
1.5	100	0.0584	0.0793	–0.3692	0.0465
	300	–0.0362	0.0704	0.2831	0.0437
	500	0.0334	0.0626	0.0681	0.0257
2	100	–0.1179	0.0762	0.3010	0.1792
	300	0.0445	0.0711	–0.2751	0.1307
	500	–0.0312	0.0702	0.1724	0.1178
2.5	100	–0.1615	0.0972	–0.2593	0.1325
	300	0.0903	0.0759	0.1722	0.1191
	500	0.0323	0.0561	–0.0433	0.1074
3.0	100	0.0941	0.7505	0.0652	0.1023
	300	–0.0644	0.0609	–0.0429	0.0912
	500	0.0565	0.0602	–0.0423	0.0885

Table 2
Bias and MSE of MLEs for different values of α with $\lambda = 2$

α	n	λ		α	
		Bias	MSE	Bias	MSE
0	100	0.0652	0.0765	–0.0813	0.0847
	300	–0.0413	0.0657	–0.0735	0.0698
	500	–0.0284	0.0583	–0.0604	0.0641
0.5	100	0.0487	0.0708	0.0349	0.0924
	300	0.0359	0.0612	–0.0262	0.0813
	500	0.0231	0.0539	–0.0188	0.0730
1	100	–0.0575	0.0674	0.1246	0.1042
	300	–0.0342	0.0553	–0.0971	0.0899
	500	–0.0271	0.0481	–0.0743	0.079
1.5	100	0.0315	0.0786	0.2641	0.1558
	300	–0.0243	0.0679	0.1932	0.1205
	500	0.0172	0.0610	0.1387	0.1036
2	100	0.1235	0.1024	–0.2184	0.1447
	300	–0.0916	0.0870	0.1713	0.1232
	500	–0.0623	0.0741	–0.1322	0.1087
2.5	100	0.0661	0.0885	0.2043	0.1360
	300	0.0512	0.0776	0.1596	0.1142
	500	0.0398	0.0684	0.1248	0.0965
3.0	100	0.0610	0.0692	–0.0567	0.0829
	300	–0.0425	0.0604	0.0412	0.0712
	500	–0.0306	0.0532	–0.0303	0.0648

Table 3
Bias and MSE of MLEs for different values of α with $\lambda = 3$

α	n	λ		α	
		Bias	MSE	Bias	MSE
0	100	–0.0711	0.0783	0.0796	0.0865
	300	0.0508	0.0680	–0.0682	0.0707
	500	0.0352	0.0605	–0.0541	0.0621
0.5	100	0.0432	0.0732	–0.0370	0.0910
	300	–0.0315	0.0627	–0.0286	0.0795
	500	0.0201	0.0548	0.0197	0.0703
1	100	–0.0534	0.0698	–0.1102	0.0992
	300	–0.0321	0.0581	–0.0887	0.0846
	500	–0.0195	0.0497	–0.0710	0.0735
1.5	100	0.0290	0.0806	0.2405	0.1421
	300	0.0218	0.0703	0.1824	0.1135
	500	0.0156	0.0635	0.1342	0.0968
2	100	0.1123	0.0974	–0.1980	0.1302
	300	–0.0875	0.0823	–0.1601	0.1103
	500	–0.0594	0.0714	–0.1256	0.0945
2.5	100	0.0583	0.0859	0.1852	0.1227
	300	0.0461	0.0750	0.1427	0.1034
	500	0.0357	0.0659	0.1096	0.0886
3.0	100	–0.0550	0.0678	–0.0501	0.0793
	300	–0.0376	0.0586	–0.0393	0.0674
	500	–0.0274	0.0524	–0.0279	0.0597

$NEExp(\alpha, \lambda)$ distribution is supported by the observed decreases in bias and MSE with increasing sample size.

6. Partially Accelerated Life Testing: A Theoretical and Simulation-Based Study of Classical and Bayesian Estimators

The following assumptions are adopted throughout this study:

1) Let n be the total number of identical and independent units, each assumed to follow the NEExp distribution, and all subjected to a life test.
2) A progressive Type-II censored sample is observed as $x_{(1)} \leq x_{(2)} \leq \cdots \leq x_{(m)}$, where m is a pre-specified number such that $m \leq n$.
3) Each unit is initially tested under normal operating conditions. If a unit neither fails nor is removed before a specified time τ, it is then subjected to accelerated (stress) conditions.
4) At the time of the i-th failure ($i = 1, 2, \ldots, m-1$), a random number R_i of the surviving units is removed from the test. Finally, at the m-th failure, the remaining surviving units, denoted as:

$$R_m = n - m - \sum_{i=1}^{m-1} R_i,$$

are all removed, and the test is terminated.

- Assume that each unit has an independent probability p of being removed at a failure time. Then, the number of units removed at each failure follows a binomial distribution:

$$R_1 \sim \text{Binomial}(n-m, p),$$

and for $i = 2, \ldots, m-1$,

$$R_i \sim \text{Binomial}\left(n - m - \sum_{j=1}^{i-1} r_j, p\right),$$

with the constraint:

$$R_m = n - m - \sum_{i=1}^{m-1} R_i.$$

The lifetime X of a unit under the Step-Stress Partially Accelerated Life Test (SS-PALT) is given by:

$$X = \begin{cases} T, \text{ if } T \leq \tau, \\ T + \frac{T-\tau}{\beta}, \text{ if } T > \tau, \end{cases} \tag{17}$$

where T represents the lifetime under normal conditions and θ, λ, and β are model parameters, with β denoting the acceleration factor. From these assumptions, the PDF of the total lifetime X is given by:

$$f(x) = \begin{cases} f_1(x) = \dfrac{\lambda(1+\alpha x^2)}{C(\alpha)} e^{-\lambda x}, 0 < x \leq \tau, \\ f_2(x) = \dfrac{\lambda(1+\alpha(\tau+\beta(x-\tau))^2)}{C(\alpha)} e^{-\lambda(\tau+\beta(x-\tau))}, x > \tau. \end{cases} \tag{18}$$

The form of $f_2(x)$ is derived using a change-of-variable technique applied to $f_1(x)$ based on the transformation in Equation (17). The probability mass function for the number of units removed at each failure is given by:

$$P(R_1 = r_1) = \binom{n-m}{r_1} p^{r_1}(1-p)^{n-m-r_1}, \; R_1 \sim \text{Binomial}(n-m, p),$$

and for $i = 2, \ldots, m-1$:

$$P(R_i = r_i | R_1 = r_1, \ldots, R_{i-1} = r_{i-1})$$
$$= (ln - m - \sum_{j=1}^{i-1} r_j r_i) p^{r_i} (1-p)^{n-m-\sum_{j=1}^{i} r_j},$$

with

$$R_i \sim \text{Binomial}\left(n - m - \sum_{j=1}^{i-1} r_j, p\right), \; R_m = n - m - \sum_{j=1}^{m-1} R_j.$$

6.1. Maximum likelihood estimation and approximate confidence intervals

This section focuses on deriving the MLEs for the population parameters and the acceleration factor under the progressive Type-II censoring scheme with binomial removals. In addition, approximate confidence intervals (ACIs) for these parameters are also established. Let $(x_i, r_i, \delta_{1i}, \delta_{2i})$ for $i = 1, 2, \ldots, m$ represent the observed data from a progressive Type-II censored (PTIIC) sample under a SS-PALT. Without loss of generality, assume the order statistics satisfy $x_{(1)} \leq x_{(2)} \leq \cdots \leq x_{(m)}$; hence, we simply write x_i instead of $x_{(i)}$ for notation convenience. Given the pre-specified number of removals $R = (R_1 = r_1, R_2 = r_2, \ldots, R_{m-1} = r_{m-1})$, the conditional likelihood function of the observed data $x = \{(x_i, r_i, \delta_{1i}, \delta_{2i}), i = 1, 2, \ldots, m\}$ is given by:

$$L_1(x_i, \Omega, \delta_{1i}, \delta_{2i} | R = r)$$
$$= \prod_{i=1}^{m} [f_1(x_i) \cdot (1 - F_1(x_i))^{r_i}]^{\delta_{1i}} [f_2(x_i) \cdot (1 - F_2(x_i))^{r_i}]^{\delta_{2i}}, \tag{19}$$

where δ_{1i} is indicator function $I(0 < x \leq \tau)$ and δ_{2i} is indicator function $I(x > \tau)$. Assuming the removals R_i are independent of the failure times X_i, the full likelihood function is:

$$L(x_i, \Omega, p) = L_1(x_i, \Omega, \delta_{1i}, \delta_{2i} | R = r) \cdot P(R = r),$$

where Ω is a vector of parameters (α, λ, β), the conditional likelihood $_1$ is simplified as:

$$L_1 \propto \lambda^{m_a} \prod_{i=1}^{m_a} (\alpha x_{(i)}^2 + 1) e^{-\lambda \sum_{i=1}^{m_a} x_{(i)}} \left(\frac{2\alpha}{\lambda^2} + 1\right)^{m_a} \prod_{i=1}^{m_a}$$
$$\left[\frac{e^{-\lambda x_{(i)}}\{\lambda^2 + \alpha(\lambda x_{(i)}(\lambda x_{(i)} + 2) + 2)\}}{2\alpha+\lambda^2}\right]^{r_i} +$$
$$\lambda^{m_b} \prod_{i=m_a+1}^{m_b} (\alpha(\tau + \beta(x_{(i)} - \tau))^2$$
$$+ 1) e^{-\lambda \sum_{i=m_a+v1}^{m_b} (\tau + \beta(x_{(i)} - \tau))} \left(\frac{2\alpha}{\lambda^2} + 1\right)^{m_b} \prod_{i=m_a+1}^{m_b}$$
$$\left[\frac{e^{-\lambda(\tau+\beta(x_{(i)}-\tau))}\{\lambda^2 + \alpha(\lambda(\tau+\beta(x_{(i)}-\tau))(\lambda(\tau+\beta(x_{(i)}-\tau)) + 2) + 2)\}}{2\alpha + \lambda^2}\right]^{r_i}. \tag{20}$$

The joint probability of the removal vector $R = r$ is given by:

$$P(R=r) = P(R_{m-1} = r_{m-1}|R_{m-2},\ldots,R_1)\cdots$$

$$P(R_2 = r_2|R_1)P(R_1 = r_1) = \frac{(n-m)!}{(n-m-\sum_{i=1}^{m-1} r_i)!\prod_{i=1}^{m-1} r_i!} p^{\sum_{i=1}^{m-1} r_i} \quad (5)$$

$$(1-p)^{(m-1)(n-m)-\sum_{i=1}^{m-1}(m-i)r_i},$$

where the total sample size is given by:

$$m = \sum_{i=1}^{m_a} \delta_{1i} + \sum_{i=1}^{m_b} \delta_{2i}.$$

The likelihood equations for the model parameters do not admit closed-form solutions. Therefore, an iterative numerical optimization method is required to obtain the maximum likelihood (ML) estimators. In this study, the estimation was carried out using the optim() function in the R software environment. Moreover, ACIs for the parameters are constructed based on the asymptotic properties of the ML estimators. These intervals are obtained by numerically inverting the observed Fisher information matrix. Hence, the approximate $100(1-\gamma)\%$ two-sided ACIs for the parameters α, λ, and β can be expressed as:

$$\widehat{\alpha} \pm z_{\gamma/2}\,\sigma_{\widehat{\alpha}},\ \hat{\lambda} \pm z_{\gamma/2}\,\sigma_{\widehat{\lambda}},\ \widehat{\beta} \pm z_{\gamma/2}\,\sigma_{\widehat{\beta}},$$

where $z_{\gamma/2}$ is the $(1-\gamma/2)$ quantile of the standard normal distribution, and $\sigma_{\widehat{\alpha}}$, $\sigma_{\widehat{\lambda}}$, and $\sigma_{\widehat{\beta}}$ denote the standard errors of the MLEs.

6.2. A Bayesian estimation approach under SELF and LINEX loss functions

In this section, we present the Bayesian estimation of the model parameters θ, λ, and the acceleration factor β for the NEExp distribution based on PTIIC data with binomial removal. The Bayesian estimation is carried out under the squared error loss function (SELF) and LINEX loss function (LLF). We assume that the prior distributions of α, λ, and β are mutually independent and follow gamma distributions. Also, the gamma prior density was first used by Degroot and Goel [26] for the parameter of acceleration factor β. Specifically, the prior densities are defined as:

$$\pi(\alpha) \propto \alpha^{a_1-1}e^{-b_1\alpha},\ \pi(\lambda) \propto \lambda^{a_2-1}e^{-b_2\lambda},$$
$$\pi(\beta) \propto \beta^{a_3-1}e^{-b_3\beta},\ a_i, b_i > 0.$$

Therefore, the joint prior density is:

$$\pi(\alpha,\lambda,\beta) \propto \alpha^{a_1-1}e^{-b_1\alpha}\lambda^{a_2-1}e^{-b_2\lambda}\beta^{a_3-1}e^{-b_3\beta}. \quad (9)$$

To specify the hyperparameters a_i and b_i for informative priors, we follow the method proposed by Dey et al. [27], in which the means and variances of the priors are matched with the MLEs and the inverse of the observed Fisher information matrix:

$$V(\alpha,\lambda,\beta) = \left[-\begin{bmatrix} \frac{\partial^2}{\partial\alpha^2} & \frac{\partial^2}{\partial\alpha\partial\lambda} & \frac{\partial^2}{\partial\alpha\partial\beta} \\ \frac{\partial^2}{\partial\lambda\partial\alpha} & \frac{\partial^2}{\partial\lambda^2} & \frac{\partial^2}{\partial\lambda\partial\beta} \\ \frac{\partial^2}{\partial\beta\partial\alpha} & \frac{\partial^2}{\partial\beta\partial\lambda} & \frac{\partial^2}{\partial\beta^2} \end{bmatrix}\right]^{-1}_{\alpha=\widehat{\alpha},\lambda=\widehat{\lambda},\beta=\widehat{\beta}}$$

Matching the mean and variance of each gamma prior yields:

$$\widehat{\alpha} = \frac{a_1}{b_1},\ V_{11} = \frac{a_1}{b_1^2},\ \hat{\lambda} = \frac{a_2}{b_2},\ V_{22} = \frac{a_2}{b_2^2},\ \widehat{\beta} = \frac{a_3}{b_3},\ V_{33} = \frac{a_3}{b_3^2}.$$

Solving gives:

$$a_1 = \frac{\widehat{\alpha}^2}{V_{11}},\ b_1 = \frac{\widehat{\alpha}}{V_{11}},\ a_2 = \frac{\hat{\lambda}^2}{V_{22}},\ b_2 = \frac{\hat{\lambda}}{V_{22}},\ a_3 = \frac{\widehat{\beta}^2}{V_{33}},\ b_3 = \frac{\widehat{\beta}}{V_{33}}.$$

Based on the conditional likelihood in Equation (3) and the joint prior in (9), the joint posterior density is:

$$\pi(\beta,\lambda,\alpha|x, R=r)$$
$$= \frac{\pi(\alpha,\lambda,\beta)\,L_1(x_i|\alpha,\lambda,\beta,R=r)}{\int_0^\infty\int_0^\infty\int_0^\infty \pi(\alpha,\lambda,\beta)\,L_1(x_i|\alpha,\lambda,\beta,R=r)\,d\alpha\,d\lambda\,d\beta}.$$

This posterior is analytically intractable; hence, we employ a Markov Chain Monte Carlo (MCMC) approach using the Metropolis–Hastings (MH) algorithm within the Gibbs sampling framework. The algorithm proceeds as follows:

1) Initialize $\Omega^{(0)} = (\alpha^{(0)},\lambda^{(0)},\beta^{(0)})$ such that $\pi(\Omega^{(0)}) > 0$.
2) For each iteration $j = 1,2,\ldots,J$ and for each parameter Ω_l:
   - Generate a candidate $\Omega_l^\times$ from a proposal distribution $q(\cdot)$.
   - Compute the acceptance probability:

$$A_l = \min\left(1, \frac{L_1(\Omega_l^\times|x,R=r)\pi(\Omega_l^\times)q(\Omega_l)}{L_1(\Omega_l|x,R=r)\pi(\Omega_l)q(\Omega_l^\times)}\right).$$

   - Generate $u \sim \text{Uniform}(0,1)$. If $u \le A_l$, accept $\Omega_l^{(j)} = \Omega_l^\times$; otherwise, set $\Omega_l^{(j)} = \Omega_l^{(j-1)}$.

3) After discarding burn-in samples, the Bayesian estimate under SELF is:

$$\widetilde{\Omega}_l = \frac{1}{J}\sum_{j=1}^{J}\Omega_l^{(j)}.$$

All computations are implemented in R, utilizing custom code for the MH algorithm combined with Gibbs sampling. In addition to the SELF, we also consider the LINEX (Linear Exponential) loss function, which is useful when overestimation and underestimation have asymmetric consequences. The LLF is defined as:

$$L(e) = c\left(e^{ae} - ae - 1\right),\ e = \widehat{\Omega}_l - \Omega_l,$$

where $a \neq 0$ is the asymmetry parameter and $c > 0$ is a scaling constant. If $a > 0$, overestimation is more costly than underestimation, and vice versa. Under the LLF, the Bayesian estimator of a parameter Ω_l is given by:

$$\widehat{\Omega}_{\text{LINEX}} = -\frac{1}{a}\log\left(\frac{1}{J}\sum_{j=1}^{J}\exp\left(-a\,\Omega_l^{(j)}\right)\right),$$

where $\{\Omega_l^{(j)}\}_{j=1}^J$ are posterior samples obtained via MCMC. This estimator is implemented in R using the same posterior draws generated by the MH within Gibbs sampling algorithm.

For each parameter (α, λ, and β), we compute both the SELF and LINEX estimators to provide a comprehensive Bayesian inference. According to Chen and Shao [28], the $100(1-\gamma)\%$ symmetric credible intervals for the parameters α, λ, and β can be constructed from the posterior samples as:

$$\left(\beta^{[M\gamma/2]},\ \beta^{[M(1-\gamma/2)]}\right),\ \left(\lambda^{[M\gamma/2]},\ \lambda^{[M(1-\gamma/2)]}\right),\ \left(\alpha^{[M\gamma/2]},\ \alpha^{[M(1-\gamma/2)]}\right),$$

where M is the number of posterior draws and the superscript $[k]$ indicates the k-th order statistic from the sorted posterior samples.

6.3. Simulation-based analysis of partially accelerated life testing methods

This section presents a comprehensive Monte Carlo simulation to evaluate and compare the performance of the proposed estimation methods for the NEExp distribution under the SS-PALT scheme with PTIIC. The estimation procedures include both maximum likelihood (ML) and Bayesian approaches. Bayesian estimates are derived using independent gamma priors under the SELF and LLF. Additionally, the simulation study is implemented using the R software environment. A major challenge in the Bayesian approach lies in deriving the posterior distributions analytically. To overcome this, the MH algorithm, combined with the Gibbs sampling scheme, is employed to generate samples from the joint posterior distributions of the parameters. The simulation process follows these main steps:

1) Generate 10,000 random samples of sizes $n = 50$ and $n = 100$ from the NEExp distribution under the SS-PALT model with PTIIC.
2) Apply the progressive Type-II censoring scheme with effective failure item counts set as:
   a. For $n = 50$: $m = 35, 45$,
   b. For $n = 100$: $m = 70, 90$.
3) Use binomial removal probabilities $p = 0.3, 0.8$.
4) Apply the uniroot() function in R to numerically invert the CDF of the NEExp distribution for simulation.
5) Consider the following sets of parameter values:
   a. **Case I** : $\alpha = 0.4, \lambda = 0.5, \beta = 1.2$),
   b. **Case II** : $\alpha = 1.9, \lambda = 0.5, \beta = 1.2$).
6) τ has been determined by quantile Q is 0.6 and 0.85.
7) For each dataset, compute the MLEs and the corresponding 95% asymptotic confidence intervals (ACIs).
8) Compute the Bayesian estimates and the associated 95% credible intervals using MCMC samples.
9) Evaluate performance using:
   a. Bias,
   b. MSE,
   c. Length of confidence or credible intervals Length of Analysis Confidence Interval (LACI) and Length of Convergence Credible Interval (LCCI).

The simulation results are summarized in Tables 4 and 5. The key findings from the simulation study are as follows:

1) For fixed n and p, increasing the number of observed failures m reduces biases, MSEs, and Length of confidence intervals (L.CIs) for all parameters in both ML and Bayesian methods.
2) For fixed m and p, increasing n improves estimation precision for all parameters.
3) For fixed n and m, increasing p generally improves estimation accuracy across all methods.
4) For fixed λ, α, and τ, increasing β decreases the bias and MSE of the estimates of λ and α, while increasing those of β.
5) For fixed n, m, p, and parameter sets, decreasing τ leads to increased bias, MSEs, and interval lengths.
6) In most scenarios, SELF demonstrates better performance than MLEs in terms of smaller biases, lower MSEs, and shorter intervals.

Table 4
The MLE and Bayesian estimation: Case I

					MLE				SELF				LLF 1			LLF 2		
n	P	Q	m		Bias	MSE	LACI	CP	Bias	MSE	LCCI	CP	Bias	MSE	LCCI	Bias	MSE	LCCI
50	10.3	0.6	35	α	0.2651	0.3431	2.0485	96.7%	0.1036	0.0392	0.5620	93.8%	0.1176	0.0446	0.5950	0.0246	0.0187	0.4860
				λ	–0.0626	0.0113	0.4050	93.3%	–0.0495	0.0026	0.1221	97.4%	–0.0494	0.0033	0.0977	–0.0505	0.0029	0.0995
				β	–0.7231	0.5508	1.2655	95.0%	–0.0713	0.0109	0.3636	92.9%	–0.0699	0.0105	0.2272	–0.0784	0.0133	0.2500
			45	α	0.1961	0.2687	1.9328	95.9%	0.0228	0.0129	0.3375	93.1%	0.0293	0.0102	0.3777	–0.0128	0.0073	0.3510
				λ	–0.0206	0.0110	0.4028	93.1%	–0.0323	0.0014	0.0891	96.8%	–0.0320	0.0014	0.0723	–0.0339	0.0016	0.0746
				β	–0.7204	0.5471	0.6237	94.8%	–0.0478	0.0070	0.1721	91.3%	–0.0472	0.0068	0.1873	–0.0511	0.0081	0.1980
		0.85	35	α	0.2315	0.3364	1.9900	97.4%	0.0674	0.0312	0.5070	91.8%	0.0802	0.0350	0.6111	–0.0053	0.0189	0.5419
				λ	–0.0050	0.0058	0.2986	93.8%	–0.0119	0.0004	0.1069	99.1%	–0.0115	0.0004	0.0589	–0.0141	0.0004	0.0583
				β	–0.6898	0.5573	1.1193	95.8%	–0.0297	0.0043	0.3493	98.2%	–0.0265	0.0044	0.1636	–0.0462	0.0057	0.1317
			45	α	0.1928	0.2667	1.8712	96.8%	0.0204	0.0109	0.3254	93.4%	0.0204	0.0100	0.3829	0.0017	0.0067	0.3515
				λ	–0.0047	0.0056	0.2863	94.9%	–0.0070	0.0002	0.0750	99.0%	–0.0068	0.0001	0.0363	–0.0081	0.0002	0.0371
				β	–0.6776	0.5442	0.6194	95.8%	–0.0193	0.0015	0.1425	98.6%	–0.0181	0.0015	0.1008	–0.0253	0.0019	0.0869
	10.8	0.6	35	α	0.2448	0.3272	2.0276	96.3%	0.0516	0.0253	0.4915	93.1%	0.0644	0.0285	0.5576	–0.0214	0.0170	0.5168
				λ	–0.0205	0.0118	0.4190	92.2%	–0.0450	0.0027	0.1248	97.6%	–0.0444	0.0026	0.1043	–0.0482	0.0030	0.1058
				β	–0.7239	0.5560	0.7014	95.1%	–0.0716	0.0117	0.2641	92.2%	–0.0702	0.0112	0.2494	–0.0789	0.0142	0.2611
			45	α	0.1693	0.2674	1.9165	95.2%	0.0213	0.0095	0.3352	92.7%	0.0277	0.0102	0.3941	–0.0132	0.0081	0.3875
				λ	–0.0163	0.0100	0.3877	93.4%	–0.0311	0.0013	0.0886	96.9%	–0.0308	0.0013	0.0683	–0.0327	0.0014	0.0697
				β	–0.7042	0.5474	0.5974	95.2%	–0.0420	0.0049	0.1671	93.4%	–0.0414	0.0048	0.1428	–0.0449	0.0057	0.1570
		0.85	35	α	0.2334	0.3117	1.9891	96.9%	0.0484	0.0317	0.5235	93.4%	0.0610	0.0274	0.5839	0.0128	0.0167	0.4971
				λ	–0.0116	0.0071	0.3271	93.9%	–0.0124	0.0004	0.1127	99.2%	–0.0119	0.0004	0.0629	–0.0148	0.0005	0.0614
				β	–0.6727	0.5341	0.6812	95.2%	–0.0336	0.0045	0.4010	98.0%	–0.0304	0.0044	0.2276	–0.0499	0.0059	0.1721

(*Continued*)

Table 4
(*Continued*)

					MLE				SELF					LLF 1			LLF 2	
n	P	Q	m		Bias	MSE	LACI	CP	Bias	MSE	LCCI	CP	Bias	MSE	LCCI	Bias	MSE	LCCI
			45	α	0.1740	0.2080	1.6535	96.1%	0.0204	0.0094	0.3593	92.7%	0.0250	0.0092	0.4183	0.0060	0.0086	0.3616
				λ	–0.0064	0.0064	0.3122	93.6%	–0.0069	0.0001	0.0754	99.4%	–0.0067	0.0001	0.0353	–0.0080	0.0002	0.0354
				β	–0.6504	0.5156	0.4859	95.3%	–0.0182	0.0017	0.2444	98.5%	–0.0170	0.0017	0.1008	–0.0247	0.0017	0.0867
2100	10.3	0.6	70	α	0.2341	0.2646	1.7962	96.7%	0.0274	0.0145	0.3915	93.4%	0.0716	0.0206	0.4181	0.0194	0.0107	0.3666
				λ	–0.0514	0.0057	0.2962	94.4%	–0.0486	0.0027	0.0881	97.7%	–0.0482	0.0027	0.0683	–0.0502	0.0029	0.0687
				β	–0.7068	0.5160	0.4507	94.3%	–0.0612	0.0087	0.1694	94.4%	–0.0606	0.0085	0.1443	–0.0640	0.0096	0.1531
			90	α	0.0995	0.1235	1.3220	96.0%	0.0120	0.0040	0.2547	95.4%	0.0157	0.0043	0.2438	–0.0074	0.0034	0.2447
				λ	–0.0118	0.0056	0.2969	94.4%	–0.0336	0.0014	0.0631	95.2%	–0.0334	0.0014	0.0588	–0.0344	0.0014	0.0604
				β	–0.7007	0.5019	0.4322	94.8%	–0.0404	0.0053	0.1116	93.9%	–0.0401	0.0052	0.1019	–0.0418	0.0058	0.1056
		0.85	70	α	0.2233	0.2531	1.7794	96.2%	0.0263	0.0139	0.3842	91.9%	0.0354	0.0157	0.4430	–0.0153	0.0112	0.4055
				λ	0.0039	0.0034	0.2291	95.3%	–0.0113	0.0002	0.0777	99.9%	–0.0111	0.0002	0.0389	–0.0125	0.0003	0.0391
				β	–0.6375	0.4876	0.4162	96.5%	–0.0320	0.0017	0.1602	99.3%	–0.0243	0.0016	0.0552	–0.0370	0.0022	0.0548
			90	α	0.1106	0.1112	1.2338	96.0%	0.0112	0.0038	0.2523	95.8%	0.0150	0.0042	0.2175	0.0026	0.0024	0.1975
				λ	–0.0020	0.0026	0.1988	96.7%	–0.0068	0.0001	0.0511	100.0%	–0.0067	0.0001	0.0196	–0.0073	0.0001	0.0196
				β	–0.6006	0.4744	0.4065	95.3%	–0.0172	0.0004	0.1094	99.7%	–0.0168	0.0004	0.0288	–0.0189	0.0005	0.0300
	10.8	0.6	70	α	0.2440	0.3144	2.0093	95.1%	0.0515	0.0190	0.4064	92.5%	0.0656	0.0213	0.4688	0.0138	0.0103	0.4012
				λ	–0.0099	0.0061	0.3050	94.2%	–0.0450	0.0028	0.0892	97.7%	–0.0495	0.0028	0.0710	–0.0514	0.0030	0.0719
				β	–0.7634	0.4965	0.4600	95.0%	–0.0614	0.0075	0.1711	94.0%	–0.0609	0.0074	0.1472	–0.0642	0.0083	0.1553
			90	α	0.0989	0.1094	1.2381	95.0%	0.0075	0.0037	0.2544	95.1%	0.0112	0.0039	0.2473	–0.0113	0.0034	0.2426
				λ	–0.0045	0.0045	0.2615	95.0%	–0.0327	0.0013	0.0630	95.9%	–0.0326	0.0013	0.0540	–0.0336	0.0014	0.0543
				β	–0.6078	0.4615	0.3870	95.6%	–0.0377	0.0051	0.1079	95.9%	–0.0374	0.0050	0.0793	–0.0389	0.0055	0.0830
		0.85	70	α	0.1704	0.2204	1.7156	95.9%	0.0190	0.0115	0.3782	94.7%	0.0266	0.0125	0.3853	–0.0216	0.0094	0.3548
				λ	0.0028	0.0039	0.2451	96.2%	–0.0118	0.0003	0.0784	99.7%	–0.0116	0.0002	0.0414	–0.0129	0.0003	0.0412
				β	–0.6563	0.4979	0.4263	95.1%	–0.0320	0.0015	0.2338	99.4%	–0.0311	0.0014	0.0574	–0.0368	0.0019	0.0537
			90	α	0.0956	0.1062	1.2216	95.9%	0.0062	0.0034	0.2501	95.7%	0.0102	0.0047	0.2330	0.0028	0.0027	0.2122
				λ	–0.0027	0.0027	0.2020	96.1%	–0.0071	0.0001	0.0518	99.7%	–0.0070	0.0001	0.0222	–0.0076	0.0001	0.0223
				β	–0.5565	0.4292	0.3567	96.0%	–0.0180	0.0007	0.1454	99.3%	–0.0176	0.0007	0.0319	–0.0198	0.0009	0.0311

Table 5
The MLE and Bayesian estimation: Case II

					MLE				SELF					LLF 1			LLF 2	
n	*P*	*Q*	*m*		Bias	MSE	LACI	CP	Bias	MSE	LCCI	CP	Bias	MSE	LCCI	Bias	MSE	LCCI
50	10.3	0.6	35	α	0.3292	1.1076	3.9205	95.9%	0.3950	0.6342	2.9404	97.0%	0.3503	0.3980	1.8181	–0.0050	0.1865	1.6663
				λ	–0.0139	0.0035	0.2257	94.1%	0.0060	0.0029	0.0970	99.5%	0.0034	0.0001	0.0300	0.0013	0.0001	0.0292
				β	0.8841	1.0737	2.1195	95.7%	0.1954	0.0648	0.9446	98.3%	0.2073	0.0715	0.5477	0.1352	0.0364	0.4531
			45	α	0.1912	0.7865	3.3964	94.2%	0.1621	0.2461	2.1923	97.4%	0.2124	0.2771	1.7487	–0.1173	0.2103	1.7392
				λ	–0.0092	0.0026	0.1990	94.9%	0.0033	0.0024	0.0684	99.6%	0.0034	0.0000	0.0167	0.0023	0.0000	0.0162
				β	0.8079	0.8834	1.8838	95.4%	0.1022	0.0205	0.6008	99.0%	0.1074	0.0223	0.2782	0.0760	0.0128	0.2430
		0.85	35	α	0.2232	0.4387	2.4456	94.7%	0.2873	0.4526	2.7402	97.3%	0.3509	0.5282	2.2060	–0.1115	0.2704	1.9690
				λ	–0.0096	0.0026	0.1972	95.1%	0.0053	0.0025	0.0867	99.9%	0.0032	0.0000	0.0251	–0.0010	0.0000	0.0241
				β	0.6824	0.8163	2.0322	96.2%	0.1807	0.0605	0.9273	98.4%	0.2035	0.0938	0.7371	0.0590	0.0354	0.6556
			45	α	0.1498	0.3983	2.4158	95.4%	0.1606	0.2371	2.1621	96.1%	0.2151	0.3127	1.8537	–0.1049	0.1837	1.6023
				λ	0.0018	0.0022	0.1858	94.3%	0.0013	0.0023	0.0601	99.7%	0.0014	0.0000	0.0133	0.0006	0.0000	0.0128
				β	0.6712	0.8063	1.8037	95.4%	0.0977	0.0201	0.5852	99.1%	0.1087	0.0294	0.3746	0.0417	0.0123	0.3102
	10.8	0.6	35	α	0.2111	0.6547	3.0635	96.7%	0.3318	0.5413	2.8608	96.7%	0.4086	0.6276	2.4932	–0.1096	0.3335	2.2240
				λ	–0.0065	0.0033	0.2237	94.9%	0.0043	0.0001	0.1004	99.5%	0.0046	0.0001	0.0339	0.0024	0.0001	0.0325
				β	0.8054	0.8870	1.9148	96.0%	0.1800	0.0564	0.9105	98.1%	0.1911	0.0619	0.5167	0.1236	0.0329	0.4349
			45	α	0.1521	0.6378	3.0070	95.1%	0.1590	0.2824	2.1981	97.3%	0.2101	0.3217	1.7656	–0.1243	0.1992	1.6890
				λ	–0.0023	0.0028	0.2063	95.7%	0.0038	0.0001	0.0695	99.3%	0.0040	0.0001	0.0201	0.0029	0.0001	0.0184
				β	0.8036	0.8697	1.8561	96.3%	0.1033	0.0177	0.6032	99.5%	0.1085	0.0193	0.2810	0.0768	0.0108	0.2368
		0.85	35	α	0.1634	0.2827	2.8444	95.5%	0.2892	0.4627	2.7928	97.1%	0.3643	0.5438	2.2648	–0.1324	0.2915	2.0165
				λ	–0.0022	0.0026	0.1980	94.6%	0.0013	0.00005	0.0884	99.9%	0.0016	0.0001	0.0256	–0.0001	0.0000	0.0241
				β	0.6303	0.7566	1.8351	96.6%	0.1655	0.0485	0.9023	98.7%	0.1871	0.0797	0.6648	0.0485	0.0309	0.5833
			45	α	0.1509	0.2791	1.9067	94.6%	0.1824	0.2983	1.9157	95.9%	0.2313	0.3399	1.8515	–0.0849	0.2097	1.7636
				λ	0.0003	0.0023	0.1869	95.7%	0.0012	0.0000	0.0601	99.7%	0.0014	0.0000	0.0130	0.0005	0.0000	0.0126
				β	0.6073	0.7089	1.7357	94.9%	0.0981	0.0162	0.5847	99.3%	0.1089	0.0245	0.2652	0.0426	0.0091	0.3269
2100	10.3	0.6	70	α	0.1930	0.4047	2.3775	95.4%	0.3267	0.5351	2.8619	97.2%	0.4045	0.6348	2.2668	–0.1100	0.2953	2.0422
				λ	–0.0076	0.0018	0.1646	94.8%	0.0041	0.00005	0.0723	100.0%	0.0043	0.0001	0.0226	0.0032	0.0000	0.0223
				β	0.8154	0.8227	1.5582	94.5%	0.1651	0.0391	0.6565	98.3%	0.1708	0.0415	0.3941	0.1362	0.0282	0.3425

(*Continued*)

Table 5
(*Continued*)

					MLE				SELF				LLF 1			LLF 2		
n	P	Q	m		Bias	MSE	LACI	CP	Bias	MSE	LCCI	CP	Bias	MSE	LCCI	Bias	MSE	LCCI
			90	α	0.1397	0.3805	2.3563	93.0%	0.1188	0.1464	1.7450	97.5%	0.1511	0.1676	1.2539	–0.0513	0.0960	1.1939
				λ	–0.0040	0.0014	0.1448	95.5%	0.0031	0.00002	0.0494	99.9%	0.0032	0.0000	0.0124	0.0026	0.0000	0.0119
				β	0.7648	0.7066	1.3683	95.8%	0.0906	0.0141	0.4188	98.7%	0.0931	0.0149	0.2038	0.0778	0.0108	0.1847
		0.85	70	α	0.1821	0.4002	2.0589	96.2%	0.2502	0.2804	2.3343	97.9%	0.3031	0.3265	1.7580	–0.0332	0.1604	1.4552
				λ	–0.0032	0.0013	0.1388	93.4%	0.0010	0.0019	0.0641	100.0%	0.0011	0.0000	0.0163	0.0002	0.0000	0.0159
				β	0.6078	0.7945	1.4252	96.5%	0.1649	0.0580	0.9623	97.8%	0.1782	0.0652	0.5830	0.0968	0.0303	0.4712
			90	α	0.1390	0.3845	1.9582	93.2%	0.1139	0.1197	1.7067	98.0%	0.1445	0.1346	1.1834	–0.0466	0.0880	1.1463
				λ	0.0011	0.0011	0.1297	95.2%	0.0009	0.00011	0.0435	99.8%	0.0012	0.0000	0.0097	0.0007	0.0000	0.0091
				β	0.5975	0.6871	1.1859	95.7%	0.0840	0.0132	0.6094	99.4%	0.0895	0.0145	0.2645	0.0562	0.0078	0.2221
	10.8	0.6	70	α	0.2015	0.6006	3.0069	94.4%	0.2885	0.4049	2.4785	97.1%	0.3478	0.4665	2.0610	–0.0371	0.2295	1.6818
				λ	–0.0032	0.0018	0.1647	93.9%	0.0046	0.0001	0.0737	100.0%	0.0048	0.0001	0.0220	0.0037	0.0000	0.0213
				β	0.7884	0.7677	1.4992	95.4%	0.1638	0.0393	0.6542	98.7%	0.1696	0.0418	0.3606	0.1349	0.0283	0.3179
			90	α	0.0833	0.3881	2.4213	92.9%	0.1104	0.1419	1.7818	97.5%	0.1442	0.1590	1.1848	–0.0679	0.1077	1.2145
				λ	–0.0022	0.0014	0.1466	95.6%	0.0036	0.00003	0.0509	99.8%	0.0037	0.0000	0.0131	0.0031	0.0000	0.0128
				β	0.7735	0.7172	1.3524	95.7%	0.0920	0.0130	0.4225	99.1%	0.0946	0.0136	0.2001	0.0790	0.0099	0.1838
		0.85	70	α	0.1539	0.2704	2.4889	95.8%	0.2586	0.3571	2.3958	96.6%	0.3154	0.4185	2.0139	–0.0562	0.1959	1.6648
				λ	–0.0020	0.0013	0.1395	94.9%	0.0008	0.00002	0.0656	99.6%	0.0010	0.0000	0.0173	0.0001	0.0000	0.0174
				β	0.5277	0.3909	1.3186	95.9%	0.1666	0.0582	0.9619	97.7%	0.1796	0.0650	0.5541	0.0996	0.0313	0.4828
			90	α	0.0715	0.1444	1.9550	93.4%	0.1063	0.1088	1.7179	97.4%	0.1372	0.1216	1.2341	–0.0580	0.0863	1.2073
				λ	0.0002	0.0011	0.1278	95.0%	0.0001	0.00001	0.0434	99.9%	0.0008	0.0000	0.0096	0.0009	0.0000	0.0093
				β	0.4744	0.2800	1.2943	96.0%	0.0820	0.0133	0.6025	99.2%	0.0874	0.0145	0.2611	0.0548	0.0081	0.2333

7) The simulation results can be reported in Tables 4 and 5.

7. Goodness of Fit in Data Modeling and Statistical Analysis

This section analyzes real-life datasets to assess the applicability and flexibility of the proposed probability distribution. A comparative study is conducted between the newly introduced model and several existing distributions, including the Pareto distribution (P), exponential distribution (Exp), and bimodal exponential distribution ($BExp$) of Reyes et al. [12]. Parameter estimation for all models is carried out using the ML method, implemented via the GenSA package in R. For model comparison, the Akaike information criterion (AIC) and Bayesian information criterion (BIC) are also employed.

7.1. Dataset I: clinical and health-related data

This application analyzes the survival times of 121 breast cancer patients from a hospital between 1929 and 1938, previously studied by Lee [29]. Figure 5 displays nonparametric plots, and Table 6 shows MLEs along with the log-likelihood, AIC, BIC,

Figure 5
Nonparametric visualization plots for Dataset I

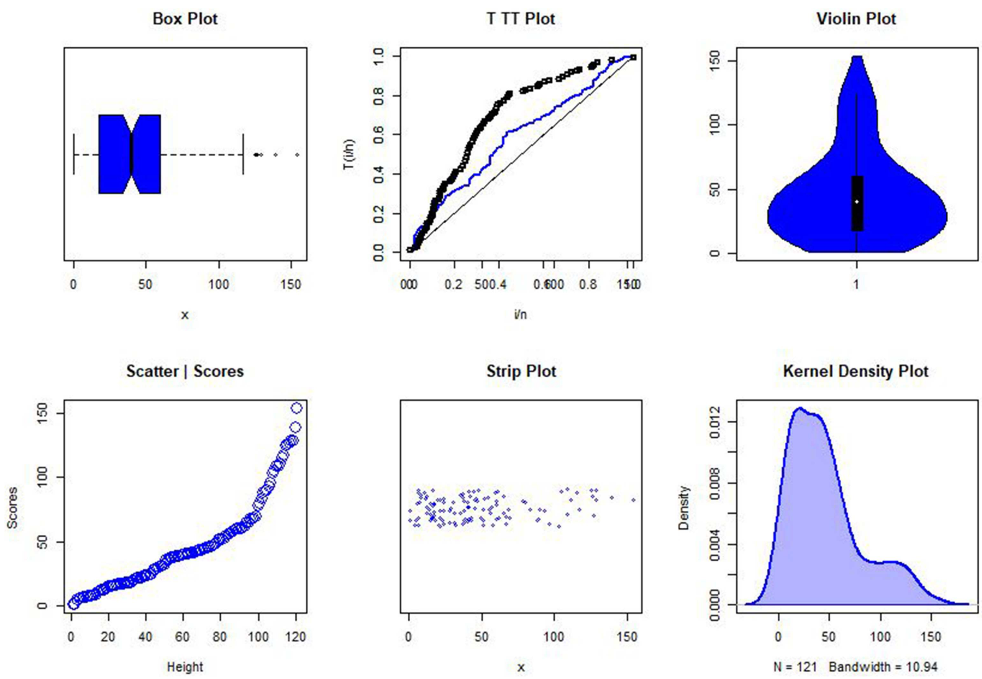

Table 6
The model comparison results for Dataset I

Distributions	Parameters				log***L***	AIC	BIC	KS
	α	λ	μ	σ				
P	—	—	0.300	0.214	–726.83	1457.66	1463.25	0.594
Exp	—	0.021	—	—	–585.12	1172.24	1175.04	0.120
BExp	0.101	0.061	—	—	–588.57	1181.14	1186.73	0.088
NEExp	0.003	0.052	—	—	–580.23	1164.46	1170.05	0.047

Figure 6
Observed and theoretical densities for Dataset I

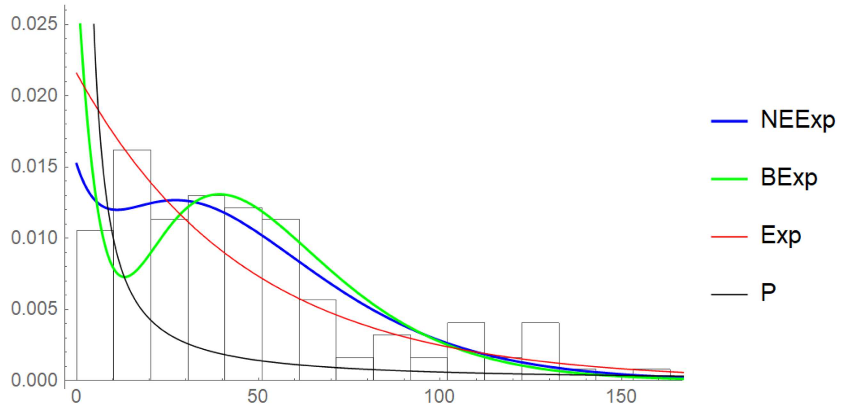

and KS statistics that go with them. The results show that the $NEExp(\alpha, \lambda)$ distribution has the lowest AIC and BIC values. Figure 6 confirms that it fits the observed data better than any other distribution.

Figure 7 displays the Q–Q and P–P plots for the breast cancer dataset under the NEEExp model. The Q–Q plot shows that the empirical quantiles align closely with the theoretical quantiles, suggesting a good fit. Similarly, the P–P plot demonstrates that the cumulative distribution follows the 45-degree line, confirming the adequacy of the model in capturing the data's distributional behavior. Besides, to prove the unique property for each estimator, the log-likelihood profiles are plotted in Figure 8. Table 7 presents the parameter estimates of the NEExp distribution based on the SS-PALT scheme using both MLE and Bayesian methods for a breast cancer dataset.

Overall, the Bayesian estimates exhibit smaller standard errors (StEr) compared to MLE, indicating higher estimation precision, particularly under shorter censoring time ($\tau = 60$) and higher removal probability ($p = 0.9$). As τ increases from 60 to 100, the standard errors generally decrease, reflecting improved estimation accuracy. The Bayesian approach consistently outperforms MLE in terms of stability and efficiency, making it more suitable for real data analysis under progressive censoring. The MCMC plots in Figure 9 illustrate the Bayesian estimation results

Figure 7
The P–P and Q–Q plots for Dataset I

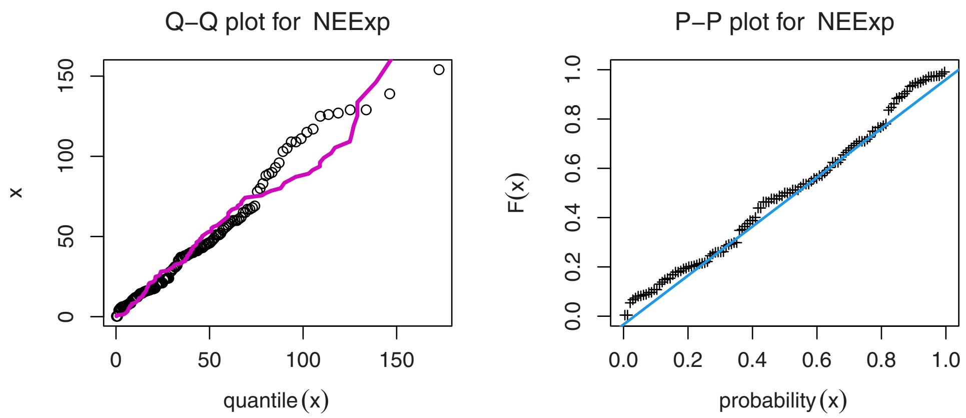

Figure 8
Log-likelihood profiles for Dataset I

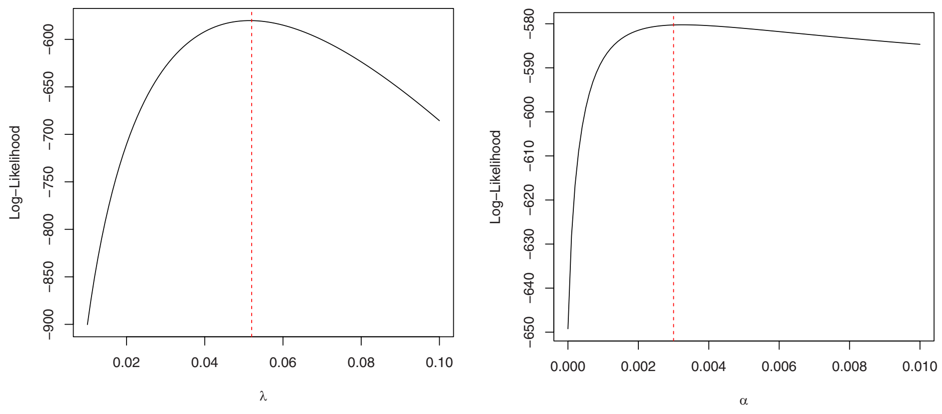

Table 7
MLE and Bayesian techniques under SS-PALT for Dataset I

τ			60				100			
			MLE		Bayesian		MLE		Bayesian	
m	p		Estimates	StEr	Estimates	StEr	Estimates	StEr	Estimates	StEr
100	0.6	α	0.0071	0.0040	0.0091	0.0039	0.0035	0.0015	0.0037	0.0014
		λ	0.0609	0.0055	0.0614	0.0047	0.0532	0.0043	0.0533	0.0040
		β	0.6962	0.1528	0.6982	0.0645	1.2532	0.1504	1.2527	0.0581
	0.9	α	0.0071	0.0040	0.0093	0.0036	0.0032	0.0012	0.0035	0.0011
		λ	0.0607	0.0055	0.0613	0.0047	0.0519	0.0041	0.0520	0.0039
		β	0.6983	0.1533	0.6996	0.0652	1.4682	0.1431	1.4782	0.0418

for the breast cancer dataset under the settings $P = 0.9$ and $\tau = 100$. For each parameter, the trace plots indicate good mixing with no apparent trends, suggesting convergence. The autocorrelation plots show a rapid decay, supporting low serial correlation. The posterior density plots are smooth and unimodal, indicating well-defined marginal posterior distributions. Overall, the diagnostics confirm reliable MCMC performance and stable posterior inference. As shown in Figure 10, the pairwise correlations of the MCMC parameters for Dataset I with $P = 0.9$ and $\tau = 100$ reveal a moderate association between p_1 and p_2, while the correlations between the other parameter pairs are weak.

7.2. Dataset II: walking dimension dataset

For this illustration, the dataset pertaining to the locations of the 68 stakes discovered while walking $L = 1000$ m and gazing $w = 20$ m on either side of the transect line is used, as previously described by Almetwally and Meraou [30]. Figure 11 shows nonparametric plots for Dataset II. The MLEs of the fitted models are shown in Table 8 together with the log-likelihood, AIC, BIC, and (KS) test statistic values that correspond to them. In the meantime, Figure 12 shows how well the fitted models work and behave. The $NEExp(\alpha, \lambda)$ distribution has lower AIC and BIC values than competing distributions, according to Table 8. Additionally, Figure 12 shows how well the $NEExp(\alpha, \lambda)$ distribution fits the data. Thus, it may be said that the distribution that fits the dataset the best is $NEExp(\alpha, \lambda)$. Table 9 shows that the Bayesian method generally provides more accurate estimates with smaller or comparable standard errors than MLE, especially for larger τ and higher p. The Bayesian approach appears more stable and reliable for the walking dimension data under the SS-PALT scheme. Figure 13 presents the Q–Q and P–P plots for the walking dimension dataset under the NEEExp model. The Q–Q plot reveals a close alignment between the empirical and theoretical quantiles, indicating a strong model fit. Likewise, the P–P plot shows the cumulative distribution adhering closely to the 45-degree line, further validating the model's ability to represent the data's distributional characteristics. In comparison, Figure 11 employs nonparametric visualizations, offering additional perspectives on the underlying data distribution. From this, it can be seen that the data show a right-skewed distribution with most values concentrated toward the lower end and a few higher outliers. Again, for showing the unique property of each estimator, the log-likelihood profiles are plotted in Figure 14. Again, Figure 15 presents MCMC diagnostics for the walking dimension dataset with $P = 0.6$ and $\tau = 8$. The trace plots show good mixing without evident trends, suggesting convergence. Autocorrelation declines gradually, indicating moderate dependence. Posterior densities are smooth and unimodal, reflecting stable posterior estimates. Overall, the MCMC algorithm performs adequately for this setting.

As shown in Figure 16, the pairwise correlations of the MCMC parameters for Dataset I with $P = 0.6$ and $\tau = 8$ reveal a moderate association between p_1 and p_2, while the correlations between the other parameter pairs are weak. Since the NEExp distribution is a direct extension of the exponential distribution, this comparison is both theoretically meaningful

Figure 9
The MCMC plots for Dataset I when P = 0.9, τ =100

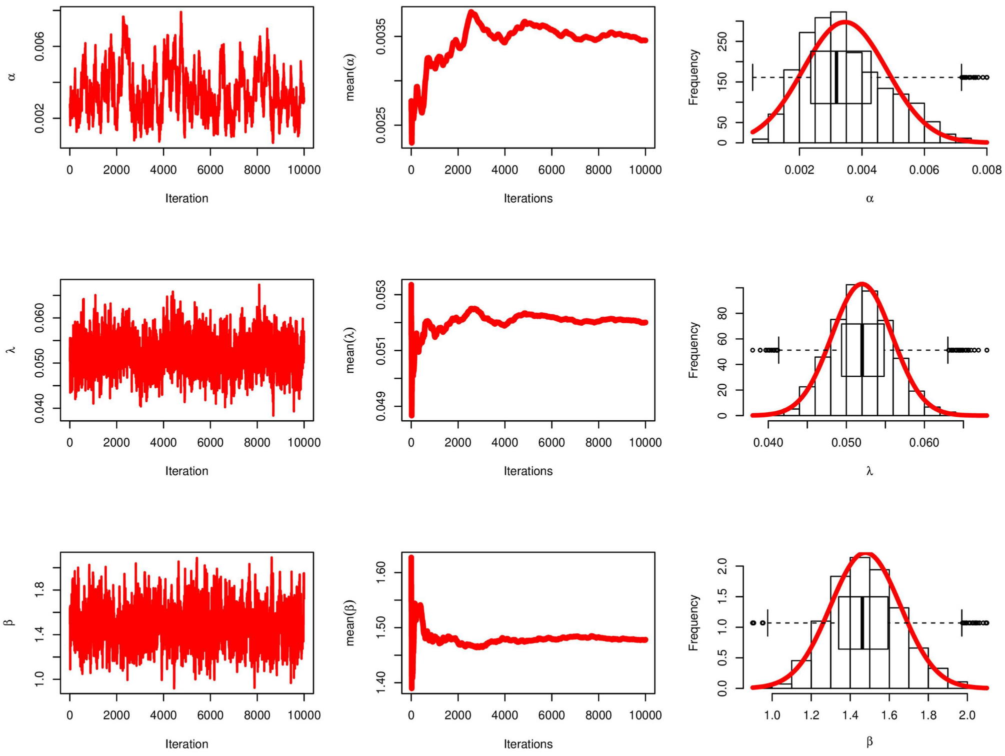

Figure 10
Pairwise correlations of MCMC parameters for Dataset I when P = 0.9, τ = 100

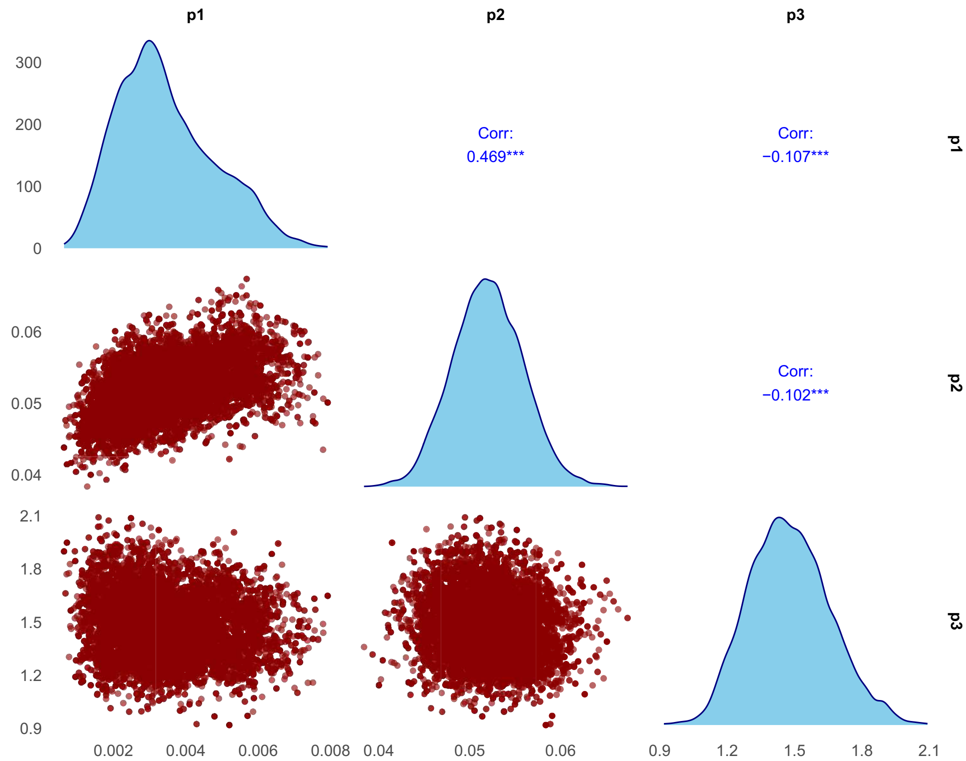

Figure 11
Nonparametric visualization plots for Dataset II

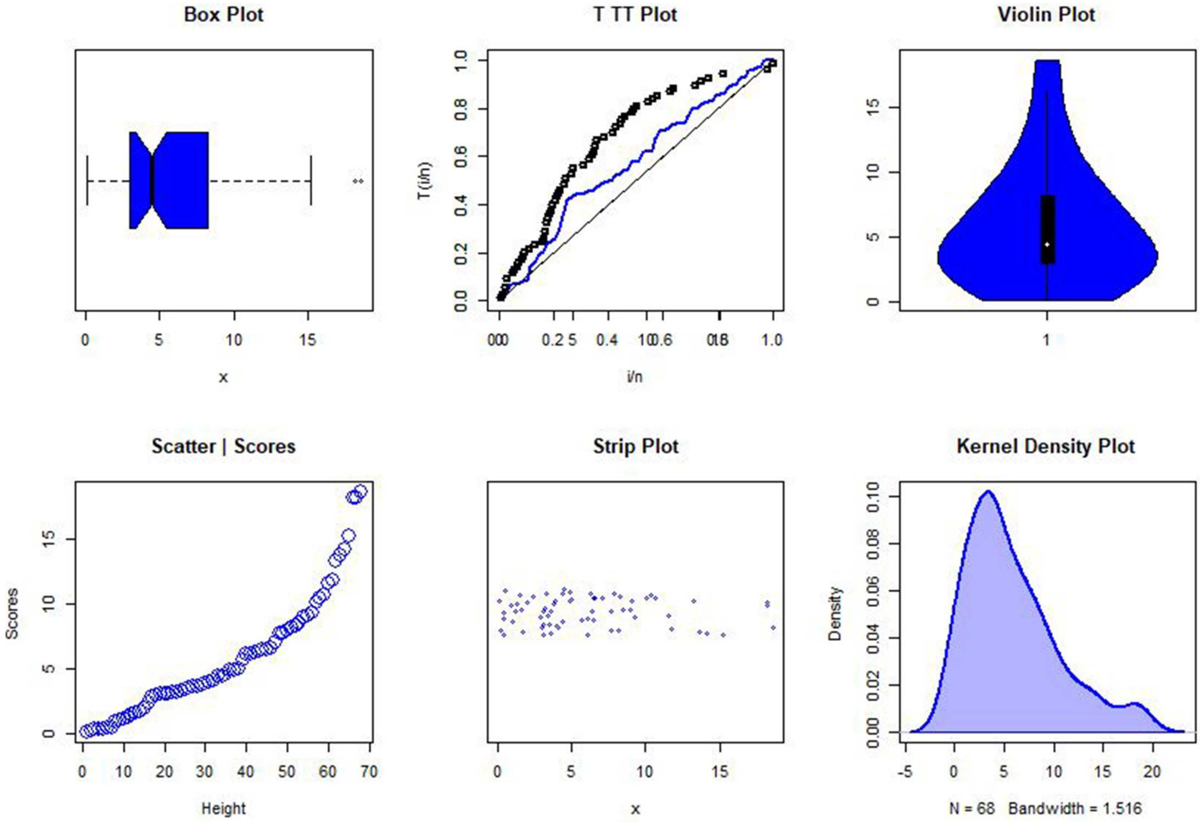

Table 8
The model comparison results for Dataset II

Distributions	Parameters				log***L***	AIC	BIC	KS
	α	λ	μ	σ				
P	—	—	0.100	0.274	–247.08	498.16	502.59	0.655
Exp	—	0.171	—	—	–188.15	378.30	380.52	0.155
BExp	0.754	0.475	—	—	–187.29	378.58	383.02	0.105
NEExp	0.147	0.394	—	—	–185.63	375.16	379.69	0.071

Table 9
The parameter's estimation based on SS-PALT for Dataset II

τ			8				10			
			MLE		Bayesian		MLE		Bayesian	
m	p		Estimates	StEr	Estimates	StEr	Estimates	StEr	Estimates	StEr
55	0.6	α	0.1513	0.1426	0.1611	0.0981	0.1123	0.0912	0.1722	0.0811
		λ	0.4150	0.0679	0.4095	0.0559	0.3882	0.0581	0.3982	0.0498
		β	0.8832	0.2839	0.9171	0.2803	1.4789	0.1864	1.6887	0.1497
	0.9	α	0.1599	0.1329	0.1904	0.1172	0.1151	0.0947	0.2943	0.0710
		λ	0.4201	0.0674	0.4180	0.0538	0.3905	0.0587	0.4130	0.0357
		β	0.8672	0.2781	0.9314	0.2784	1.4690	0.0859	1.7674	0.0793

Figure 12
Observed and theoretical densities for Dataset II

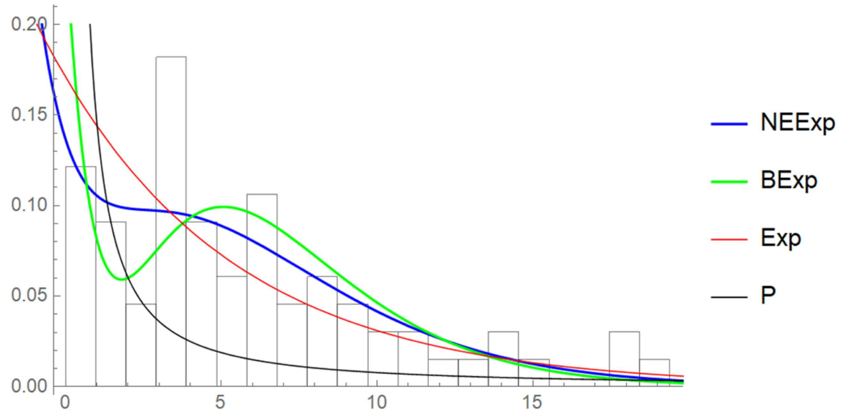

Figure 13
The P–P and Q–Q plots for Dataset II

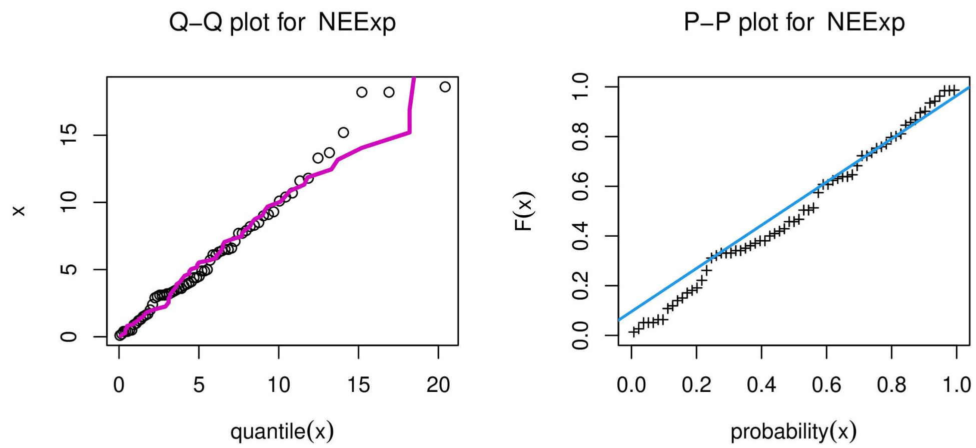

Figure 14
Log-likelihood profiles for Dataset II

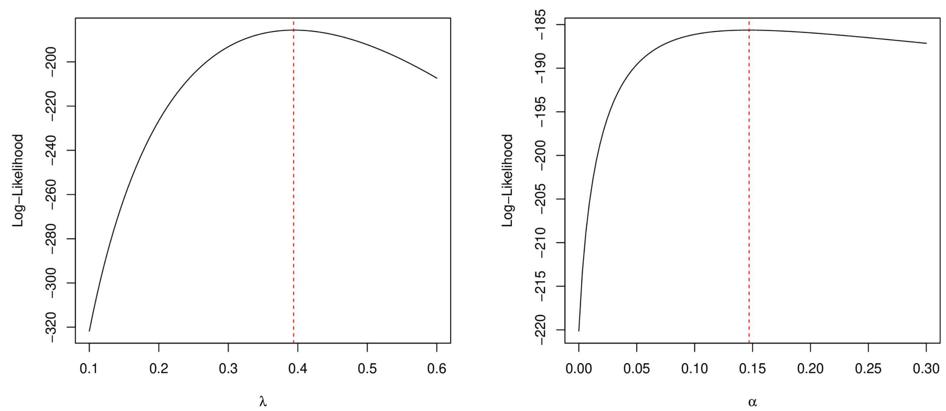

and sufficient to demonstrate the advantages of the proposed model. The results from both simulation studies and real data applications indicate that the NEExp model consistently provides a better fit, particularly in datasets exhibiting asymmetry, varying dispersion, and non-constant hazard rate structures. In contrast, the classical exponential distribution, due to its constant hazard rate assumption, fails to capture such complex behaviors. The additional shape parameter in the NEExp model allows for greater flexibility, enabling it to accommodate unimodal as well as bimodal patterns observed in practical data. Therefore, the improved performance of the proposed model over its baseline counterpart substantiates its applicability in reliability and survival analysis without necessitating comparisons with structurally unrelated distributions.

Figure 15
The MCMC plots for Dataset II when P = 0.6, τ=8

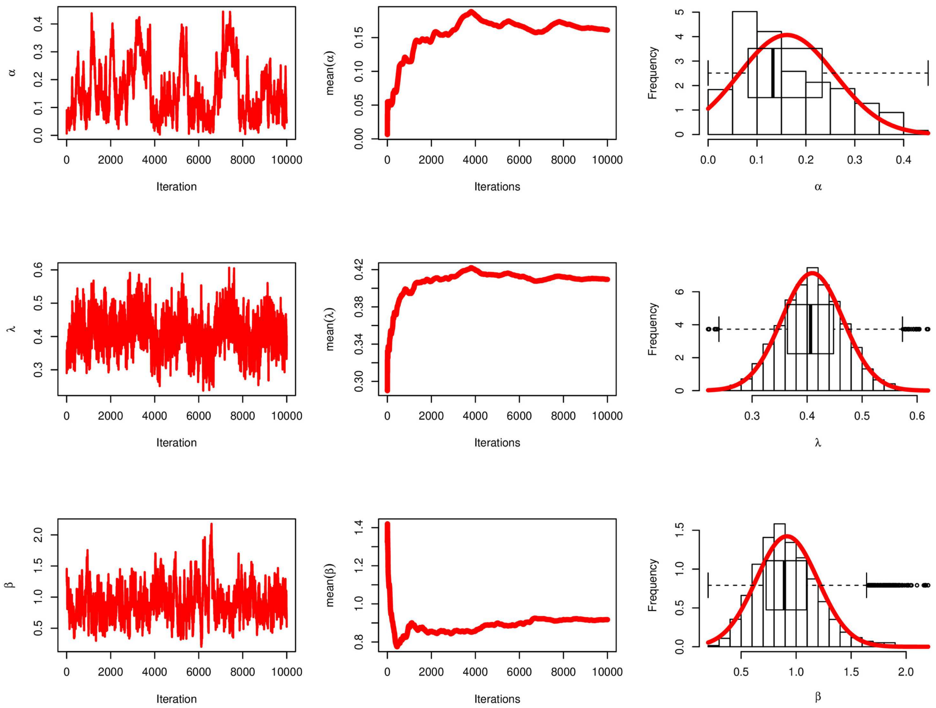

Figure 16
Pairwise correlations of MCMC parameters for Dataset II when P = 0.6, τ=8

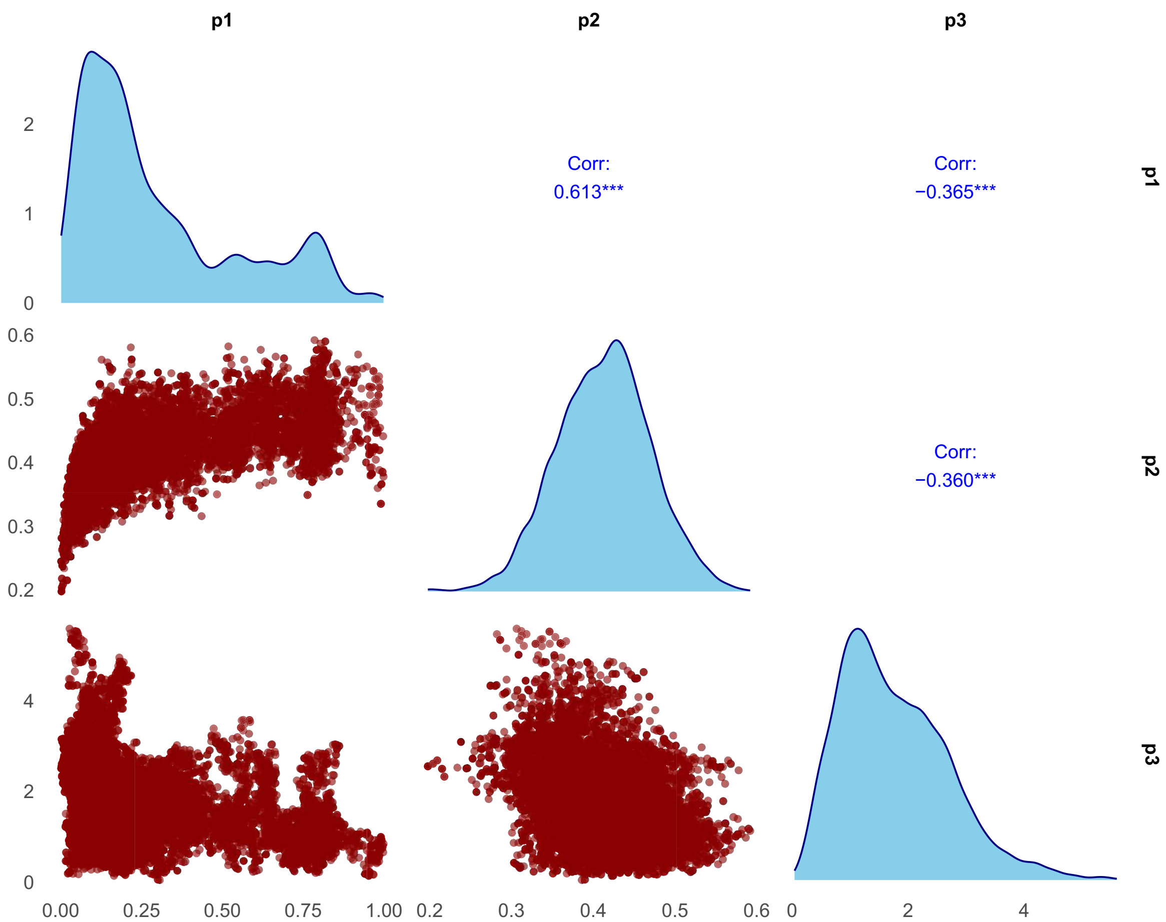

Table 10
Result of LRT for Datasets I and II

	Statistic value		Critical value
Hypothesis	Data I	Data II	
$H_0 : \alpha = 0$ Vs $H_1 : \alpha \neq 0$	9.78	6.28	3.841

7.3. Comparative likelihood ratio analysis of Datasets I and II

In this section, the LRT is used to discriminate between the *NEExp* distribution and its nested models. For this analysis, the test statistic and the null hypothesis are discussed below. The null hypothesis is given as follows:

$$H_0 : \alpha = 0,$$

must be tested against the alternative hypothesis

$$H_1 : \alpha \neq 0,$$

in order to distinguish the *Exp* distribution from the *NEExp* distribution. The test statistic is given by

$$-2\log(LR) = -2\left[\log L(\hat{\lambda}_1, \alpha = 0|x) - \log L(\hat{\alpha}_2, \hat{\lambda}_2|x)\right] \sim \chi_1^2,$$

where $r = 1$ is the difference between the numbers of parameters and $\hat{\lambda}_1$ and $(\hat{\alpha}_2, \hat{\lambda}_2)$ are the MLEs of the *Exp* and *NEExp* distributions, respectively.

From Table 10, it is observed that the LRT statistic exceeds the tabulated critical value at the 95% confidence level for both Dataset I and Dataset II. Therefore, the null hypothesis is rejected, and it can be concluded that the data are well-modeled by the *NEExp* distribution.

8. Conclusion and Future Scope of the Study

This study introduced a novel extension of the exponential distribution, referred to as the NEExp distribution, designed to provide enhanced flexibility in modeling non-negative data exhibiting both unimodal and bimodal characteristics. By incorporating a shape-controlling parameter, the proposed model successfully overcomes the limitations of the classical exponential distribution, particularly its inability to capture varying hazard rate behaviors and complex data structures. A comprehensive theoretical framework was developed for the NEExp distribution, including explicit derivations of its PDF, CDF, MGF, raw moments, entropy measures, and reliability characteristics. The model was shown to accommodate a wide range of hazard rate shapes, including increasing and bathtub forms, making it particularly suitable for applications in reliability engineering and survival analysis. Furthermore, several characterization results based on truncated moments, hazard functions, and conditional expectations were established, strengthening the theoretical foundation of the proposed model. From an inferential perspective, both classical and Bayesian estimation methods were explored. MLE was implemented using numerical optimization techniques, and its performance was assessed through extensive simulation studies. The results demonstrated that the estimators are consistent and efficient, with decreasing bias and MSE as the sample size increases. In addition, Bayesian estimation under both symmetric (SELF) and asymmetric (LINEX) loss functions was developed using MCMC methods, providing flexible and robust alternatives for parameter estimation under complex sampling schemes. The applicability of the NEExp distribution was further extended to PALT models under progressive Type-II censoring with binomial removals. This framework reflects realistic experimental conditions and allows for efficient reliability assessment in time-constrained environments. Simulation results confirmed the effectiveness of both classical and Bayesian approaches in such settings, highlighting the practical relevance of the proposed model. Despite its flexibility and strong theoretical properties, the proposed NEExp distribution has certain limitations that should be acknowledged. First, the estimation procedures, particularly under the Bayesian framework, rely on computationally intensive techniques such as the MH algorithm within Gibbs sampling. This may lead to increased computational burden, especially for large datasets or complex censoring schemes. Second, the numerical optimization required for MLE depends on initial parameter values, and poor initialization may affect convergence or lead to local optima. Additionally, while the model introduces greater flexibility through the shape parameter, this may also increase sensitivity to parameter estimation errors, particularly in small samples. From an application standpoint, although the model has demonstrated strong performance in reliability and survival contexts, its applicability to other domains such as financial risk modeling, environmental data analysis, and biomedical signal processing requires further empirical validation. Future research may focus on developing more efficient estimation algorithms, exploring robust estimation techniques, and extending the model to multivariate or regression-based frameworks. Investigating goodness-of-fit measures, model selection criteria, and real-time implementation strategies would also enhance its practical usability across a broader range of disciplines.

Funding Support

This work was supported and funded by the Deanship of Scientific Research at Imam Mohammad Ibn Saud Islamic University (IMSIU) (Grant Number IMSIU-DDRSP2601).

Ethical Statement

This study utilized publicly available, fully de-identified datasets from previously published research (Lee [29]; Almetwally and Meraou [30]). Because the data are sourced from open-access literature, ethical approval and informed consent were not required.

Conflicts of Interest

The authors declare that they have no conflicts of interest to this work.

Data Availability Statement

The data that support the findings of this study are openly available at https://doi.org/10.1109/TR.1986.4335370, reference number [29], and at https://doi.org/10.21608/cjmss.2022.271186, reference number [30].

Author Contribution Statement

Mohamed S. Eliwa: Methodology, Software, Formal analysis, Investigation, Data curation, Writing – original draft, Writing – review & editing, Supervision, Project administration. **Mohamed F. Abouelenein:** Software, Validation, Investigation, Resources, Data curation, Writing – original draft, Writing – review & editing, Visualization, Funding acquisition. **Jondeep Das**: Conceptualization, Methodology, Software, Validation, Resources, Data curation, Writing – original draft, Writing – review & editing, Visualization. **Lakhimi Doley:** Conceptualization, Methodology, Formal analysis, Investigation, Data curation, Writing – original draft, Writing – review & editing. **Partha Jyoti Hazarika:** Conceptualization, Methodology, Software, Validation, Formal analysis, Investigation, Resources, Data curation, Writing – original draft, Writing – review & editing, Visualization, Supervision, Project administration. **Gholamhossein G. Hamedani:** Methodology, Software, Investigation, Data curation, Writing – original draft, Writing – review & editing, Visualization. **Ehab M. Almetwally:** Methodology, Resources, Data curation, Software, Writing – review & editing.

References

[1] Alkhazaleh, M., Alkhazaleh, S., Handam, A., Abu-Saleem, A., & Alkhazaleh, A. M. H. (2024). Extended exponential distribution with application on financial data. *Applied Mathematics & Information Sciences*, *18*(6), 1455–1467. http://doi.org/10.18576/amis/180622

[2] Ragab, I. E., Alsadat, N., Balogun, O. S., & Elgarhy, M. (2024). Unit extended exponential distribution with applications. *Journal of Radiation Research and Applied Sciences*, *17*(4), 101118. https://doi.org/10.1016/j.jrras.2024.101118

[3] Khaoula, A., Seddik-Ameur, N., Ahmad, A. E.-B. A., & Khaleel, M. A. (2022). The Topp-Leone extended exponential distribution: Estimation methods and applications. *Pakistan Journal of Statistics and Operation Research*, *18*(4), 817–836. https://doi.org/10.18187/pjsor.v18i4.3699

[4] Eliwa, M. S., Alshammari, F. S., Abualnaja, K. M., & El-Morshedy, M. (2021). A flexible extension to an extreme distribution. *Symmetry*, *13*(5), 745. https://doi.org/10.3390/sym13050745

[5] El-Morshedy, M. (2024). Classical and Bayesian techniques for modelling engineering dataset using new generalized probability distribution with mathematical features. *Applied Mathematics & Information Sciences*, *18*(4), 715–730. http://dx.doi.org/10.18576/amis/180404

[6] Eliwa, M. S., & El-Morshedy, M. (2025). A discrete extension of the exponential type II distribution: Statistical characterizations, reliability analysis, and Bayesian vs. non-Bayesian inferences for random right-censored and complete count data. *Japanese Journal of Statistics and Data Science*, *8*(1), 279–317. https://doi.org/10.1007/s42081-024-00277-8

[7] Qayoom, D., Rather, A. A., Volodin, A., Supapueng, O., Khan, A. H., & Danish, F. (2025). DUS exponential distribution: Properties and applications. *Lobachevskii Journal of Mathematics*, *46*(10), 5213–5228. https://doi.org/10.1134/S199508022560966X

[8] Shukr, B. A. (2026). An improved extension of unit moment exponential distribution: Mathematics, inference, and applications. *Mathematical Sciences*, *20*(1), 73–89. https://doi.org/10.57647/mathsci.2026.85781

[9] Ibrahim, M., Hamedani, G. G., Al-Nefaie, A. H., & Yousof, H. M. (2026). Distributional analysis and risk assessment of UK motor non-comprehensive claims using the log-exponential family with properties and characterizations. *Statistics, Optimization and Information Computing*, *15*(5), 3630–3654. https://doi.org/10.19139/soic-2310-5070-3451

[10] El Gazar, A. M., Metwally, D. S., Elgarhy, M., & El-Desouky, B. S. (2026). Truncated transmuted exponential distribution with different estimation methods and applications. *Journal of Multidisciplinary Applied Natural Science*, *6*(1), 19–43. https://doi.org/10.47352/jmans.2774-3047.306

[11] Bar-Lev, S. K., & Ridder, A. (2025). New exponential dispersion models for count data–A review and applications. In S. Bersimis, P. Economou, & A. Rakitzis (Eds.), *Statistical methods and applications in systems assurance and quality* (pp. 245–266). CRC Press. https://doi.org/10.1201/9781032664330-12

[12] Reyes, J., Gómez-Déniz, E., Gómez, H. W., & Calderín-Ojeda, E. (2021). A bimodal extension of the exponential distribution with applications in risk theory. *Symmetry*, *13*(4), 679. https://doi.org/10.3390/sym13040679

[13] Reyes, J., Arnold, B. C., Gómez, Y. M., Venegas, O., & Gómez, H. W. (2025). Modified bimodal exponential distribution with applications. *Axioms*, *14*(6), 461. https://doi.org/10.3390/axioms14060461

[14] Alzaghal, A., Aldeni, M., & Al-Aqtash, R. (2023). A new class of exponentiated exponential distributions: Bimodality, regression, and application. *Journal of Statistical Theory and Practice*, *17*(4), 52. https://doi.org/10.1007/s42519-023-00349-0

[15] Rodrigues, G. M., Ortega, E. M. M., Vila, R., Cordeiro, G. M., & Cóndor, C. M. R. (2026). An extended normal distribution for skewed and bimodal data: New properties and a new regression model. *Communications in Statistics - Theory and Methods*, *55*(6), 1888–1905. https://doi.org/10.1080/03610926.2025.2538538

[16] Homayouni, M., Khaledi, M. J., Najafi, E., & Sohrabi, H. (2026). Generalized spatial beta models for skewed and bimodal proportion data. *Computational Statistics*, *41*(1), 3. https://doi.org/10.1007/s00180-025-01701-7

[17] de Moura, G. L. S., de Souza Neto, T. A., Cecon, P. R., Filho, S. M., & Carneiro, A. P. S. (2025). Bayesian implementation of Skew-Normal distributions for experimental error in the description of pepper growth. *Brazilian Journal of Biometrics*, *43*(2), e43726. https://doi.org/10.28951/bjb.v43i2.726

[18] Elal-Olivero, D., Olivares-Pacheco, J. F., Venegas, O., Bolfarine, H., & Gómez, H. W. (2020). On properties of the bimodal skew-normal distribution and an application. *Mathematics*, *8*(5), 703. https://doi.org/10.3390/math8050703

[19] Alomani, G. A., Hassan, A. S., Al-Omari, A. I., & Almetwally, E. M. (2024). Different estimation techniques and data analysis for constant-partially accelerated life tests for power half-logistic distribution. *Scientific Reports*, *14*(1), 20865. https://doi.org/10.1038/s41598-024-71498-w

[20] Lv, S., Li, F., Wang, G., & Li, S. (2024). Bayesian analysis of accelerated life test under constrained randomization. *Quality*

Engineering, *36*(1), 105–117. https://doi.org/10.1080/08982112.2023.2255899

[21] Hassan, A. S., & Elghaffar, A. M. A. (2025). Bayesian and e-Bayesian estimation of Gompertz distribution in stress-strength reliability model under partially accelerated life testing. *Computational Journal of Mathematical and Statistical Sciences*, *4*(1), 348–378. https://doi.org/10.21608/cjmss.2025.353923.1107

[22] Rabie, A., Hussam, E., Muse, A. H., Aldallal, R. A., Alharthi, A. S., & Aljohani, H. M. (2022). Estimations in a constant-stress partially accelerated life test for generalized Rayleigh distribution under Type-II hybrid censoring scheme. *Journal of Mathematics*, *2022*(1), 6307435. https://doi.org/10.1155/2022/6307435

[23] Glanzel, W. (1990). Some consequences of a characterization theorem based on truncated moments. *Statistics*, *21*(4), 613–618. https://doi.org/10.1080/02331889008802273

[24] Hamedani, G. G. (2013). On generalized gamma convolution distributions. *Journal of Applied Mathematics, Statistics and Informatics*, *9*(1), 5–14. https://doi.org/10.2478/jamsi-2013-0001

[25] Das, J., Hazarika, P. J., Chakraborty, S., Pathak, D., Hamedani, G. G., & Karamikabir, H. (2024). A bimodal extension of the Tanh Skew Normal distribution: Properties and applications. *Pakistan Journal of Statistics and Operation Research*, *20*(3), 533–551. http://doi.org/10.18187/pjsor.v20i3.4563

[26] Degroot, M. H., & Goel, P. K. (1979). Bayesian estimation and optimal designs in partially accelerated life testing. *Naval Research Logistics Quarterly*, *26*(2), 223–235. https://doi.org/10.1002/nav.3800260204

[27] Dey, S., Singh, S., Tripathi, Y. M., & Asgharzadeh, A. (2016). Estimation and prediction for a progressively censored generalized inverted exponential distribution. *Statistical Methodology*, *32*, 185–202. https://doi.org/10.1016/j.stamet.2016.05.007

[28] Chen, M.-H., & Shao, Q.-M. (1999). Monte Carlo estimation of Bayesian credible and HPD intervals. *Journal of Computational and Graphical Statistics*, *8*(1), 69–92. https://doi.org/10.1080/10618600.1999.10474802

[29] Lee, E. T. (1986). Statistical methods for survival data analysis. *IEEE Transactions on Reliability*, *35*(1), 123–123. https://doi.org/10.1109/TR.1986.4335370

[30] Almetwally, E. M., & Meraou, M. A. (2022). Application of environmental data with new extension of Nadarajah-Haghighi distribution. *Computational Journal of Mathematical and Statistical Sciences*, *1*(1), 26–41. https://doi.org/10.21608/cjmss.2022.271186

How to Cite: Eliwa, M. S., Abouelenein, M. F., Das, J., Doley, L., Hazarika, P. J., Hamedani, G. G., & Almetwally, E. M. (2026). An Innovative Exponential Distribution for Modeling Various Risk Trends: Theory, Bayesian Inference, and Applications in Partially Accelerated Life Tests with Dispersion Data. *Journal of Computational and Cognitive Engineering*, *5*(3), 438–462. https://doi.org/10.47852/bonviewJCCE62027466